

Pervasive cranial allometry at different anatomical scales and variational levels in extant armadillos

Alometría craneal generalizada a diferentes escalas anatómicas y niveles de variación en armadillos actuales

Kévin Le Verger^{1,2}, Lionel Hautier^{3,4}, Sylvain Gerber⁵, Jérémie Bardin⁶, Frédéric Delsuc³, Laureano R. González Ruiz⁷, Eli Amson⁸, Guillaume Billet²

¹Department of Paleontology, University of Zurich, Zurich, Switzerland

²Museum national d'Histoire naturelle, The Origins and Evolution Department, Centre de Recherche en Paléontologie—Paris, UMR 7207 CR2P MNHN/CNRS/UPMC, Sorbonne Universités, Paris, France (MNHN)

³Institut des Sciences de l'Evolution, Environmental changes, spatio-temporal dynamics, eco-evolution department, Université de Montpellier, UMR 5554 ISEM CNRS/IRD/EPHE, Montpellier cedex, France

⁴Natural History Museum of London, Mammal Section, Department of Life Sciences, London, United Kingdom

⁵Museum national d'Histoire naturelle, The Origins and Evolution Department, Institut de Systématique, Évolution, Biodiversité, UMR 7205 ISYEB MNHN/CNRS/UPMC/EPHE, Sorbonne Universités, Paris, France

⁶Museum national d'Histoire naturelle, The Origins and Evolution Department, Centre de Recherche en Paléontologie—Paris, UMR 7207 CR2P MNHN/CNRS/UPMC, Sorbonne Universités, Paris, France (UPMC)

⁷Laboratorio de Investigaciones en Evolución y Biodiversidad (LIEB-FCNyCS sede Esquel, UNPSJB) y Centro de Investigaciones Esquel de Montaña y Estepa Patagónica (CIEMEP), CONICET, Universidad Nacional de La Patagonia San Juan Bosco (UNPSJB), Chubut, Argentina

⁸Staatliches Museum für Naturkunde, Stuttgart, Germany

Corresponding author: Department of Paleontology, University of Zurich, Karl-Schmid-Strasse 4, 8006 Zurich, Switzerland. Email: kevin.leverger@pim.uzh.ch

Abstract

Allometry, i.e., morphological variation correlated with size, is a major pattern in organismal evolution. Since size varies both within and among species, allometry occurs at different variational levels. However, the variability of allometric patterns across levels is poorly known since its evaluation requires extensive comparative studies. Here, we implemented a 3D geometric morphometric approach to investigate cranial allometry at three main variational levels—static, ontogenetic, and evolutionary—and two anatomical scales—entire cranium and cranial subunits—based on a dense intra- and interspecific sampling of extant armadillo diversity. While allometric trajectories differ among distantly related species, they hardly do so among sister families. This suggests that phylogenetic distance plays an important role in explaining allometric divergences. Beyond trajectories, our analyses revealed pervasive allometric shape changes shared across variational levels and anatomical scales. At the entire cranial scale, craniofacial allometry (relative snout elongation and braincase reduction) is accompanied notably by variations of nuchal crests and postorbital constriction. Among cranial subunits, the distribution of allometry was highly heterogeneous, with the frontal and petrosal bones showing the most pervasive shape changes, some of which were undetected at a more global scale. Evidence of widespread and superimposed allometric variations raises questions on their determinants and anatomical correlates and demonstrates the critical role of allometry in morphological evolution.

Resumen

La alometría, es decir, la variación morfológica correlacionada con el tamaño, es un patrón importante en la evolución de los organismos. Dado que el tamaño varía tanto dentro de las especies como entre ellas, la alometría se produce en distintos niveles variacionales. Sin embargo, la variabilidad de los patrones alométricos entre niveles es poco conocida, ya que su evaluación requiere amplios estudios comparativos. En este trabajo hemos implementado un enfoque morfométrico geométrico en 3D para investigar la alometría craneal en tres niveles variacionales principales -estático, ontogenético y evolutivo- y en dos escalas anatómicas -cráneo completo y subunidades craneales- basándonos en un denso muestreo intra e interespecífico de la diversidad de armadillos existentes. Mientras que las trayectorias alométricas difieren entre especies distantemente emparentadas, apenas lo hacían entre familias hermanas. Esto sugiere que la distancia filogenética desempeña un papel importante a la hora de explicar las divergencias alométricas. Más allá de las trayectorias, nuestros análisis revelaron cambios alométricos generalizados en la forma, compartidos a través de niveles variacionales y escalas anatómicas. En toda la escala craneal, la alometría craneofacial (alargamiento relativo del hocico y reducción de la caja encefálica) se acompaña notablemente de variaciones de las crestas nucales y la constricción postorbital. Entre las subunidades craneales, la distribución de la alometría era muy heterogénea, siendo los huesos frontal y petroso los que mostraban los cambios de forma más generalizados, algunos de los cuales no se detectaban a una escala más global. La evidencia de variaciones alométricas generalizadas y superpuestas plantea interrogantes sobre sus determinantes y correlatos anatómicos y demuestra el papel crítico de la alometría en la evolución morfológica.

Keywords: size, evolutionary level, intraspecific level, cranium, cranial subunits, cingulata

Received April 24, 2023; revisions received November 27, 2023; accepted December 6, 2023

Associate Editor: Kjetil Voje; Handling Editor: Miriam Zelditch

© The Author(s) 2023. Published by Oxford University Press on behalf of The Society for the Study of Evolution (SSE).

This is an Open Access article distributed under the terms of the Creative Commons Attribution-NonCommercial License (<https://creativecommons.org/licenses/by-nc/4.0/>), which permits non-commercial re-use, distribution, and reproduction in any medium, provided the original work is properly cited. For commercial re-use, please contact journals.permissions@oup.com

Introduction

The concept of allometry describes the variation of organismal traits associated with size. This phenomenon constitutes a pervasive pattern (e.g., Gould, 1966; Hallgrímsson et al., 2019; Klingenberg, 1996) found at multiple variational levels: (a) static, a single ontogenetic stage within a species; (b) ontogenetic, several ontogenetic stages within a single species; and (c) evolutionary, a single ontogenetic stage in several species (Cheverud, 1982a; Klingenberg, 1996). Allometric variation is also present at various anatomical scales in the body (Le Verger et al., 2020), which makes shape—size covariation inherently complex. Such complexity originates from a highly polygenic source (Hallgrímsson et al., 2019; Klingenberg, 2010; Pélabon et al., 2014; Zelditch et al., 2003) and multiple developmental and evolutionary processes intertwined with morphological integration (Klingenberg, 2014; Zelditch & Goswami, 2021). The wide expression of allometry implies that variation in size might drive evolutionary trends or constrain morphological variation (Gould, 1989; Klingenberg, 2016; Klingenberg & Marugán-Lobón, 2013; Sidlauskas,

2008; Zelditch & Swiderski, 2022). Allometric trajectories or shape changes can even be biological traits under selection (Adams & Nistri, 2010; Giannini, 2014; Klingenberg, 2010; Porto et al., 2013; Urošević et al., 2013).

Traditionally, allometry is examined either at the intraspecific level, for which the two main variational levels are the static and the ontogenetic levels (Figure 1). Usually, ontogenetic allometric trajectories are independently documented to test if similarities can be detected in more or less distant species (e.g., Adams & Nistri, 2010; Esquerré et al., 2017; Ferreira-Cardoso et al., 2019; Piras et al., 2011; Simons & Frost, 2020; Weston, 2003; Wilson, 2018; Zelditch et al., 2003). The evolutionary approach involves testing whether shape changes could be related to size variation across a clade (see Klingenberg & Marugán-Lobón, 2013; and citations therein). As size variation among species is substantial, allometry can explain a large part of the morphological variation at the evolutionary level. This approach is crucial for highlighting widespread evolutionary patterns (e.g., Cardini, 2019a; Billet & Bardin, 2021; Giannini et al., 2021).

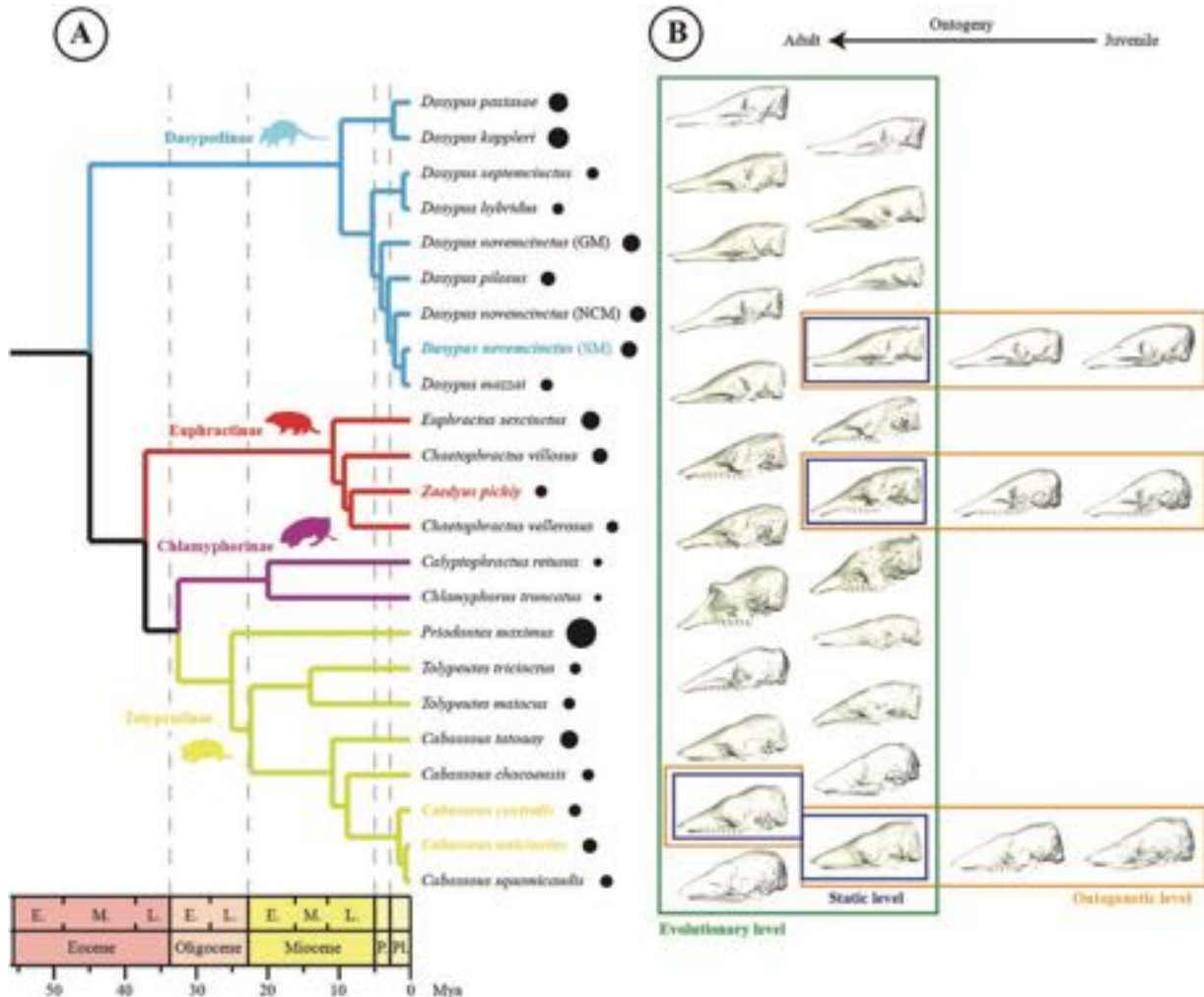


Figure 1. Phylogenetic context, sample, and variational levels. (A) Time-calibrated phylogeny of the sampled taxa (reconstructed from Feijó et al., 2019; Gibb et al., 2016). The diameter of the black circle for each taxon is proportional to cranial adult size (centroid size). Species name in bold represent those species sampled at intraspecific levels. (B) Levels of variation sampled in this study: species sampled at intraspecific levels (ontogenetic and static) are represented by a series of crania at different developmental stages, while species sampled for the evolutionary level only are represented by a single adult cranium (see text for further explanation and for the special case of *Cabassous*). Abbreviations: E, early; M, middle; Mya, million years ago; L, late.

As with the study of integration and modularity (Klingenberg, 2014), multilevel comparative studies can enhance our global understanding of allometric variation within a clade. The primary benefit of comparing the shape changes at the intraspecific and evolutionary levels is to provide details on the extent of the observed variation (Evans et al., 2022; Klingenberg, 2014; Zelditch & Goswami, 2021). Comparing different levels is also beneficial in that studies that look for allometric correlations at the evolutionary level alone can be misled by unreplicated evolutionary events (Uyeda et al., 2018), while intraspecific studies alone cannot inform on patterns between species. Similarities between these two variational levels can lend further support for recognized novel patterns of evolutionary allometry (e.g., Cardini & Polly, 2013). However, comparisons of allometric shape changes are rarely undertaken, especially with the use of 3D geometric morphometric methods (GMMs), and the maintenance of allometric shape changes across levels of variation remains understudied.

In addition to the three classical variational levels, the scrutiny and comparison of patterns of variation at different anatomical scales may also be valuable to better understand allometry. Body parts are often arranged hierarchically in organisms, so that different anatomical scales may be recognized for a wide variety of organs. The mammalian cranium is a classic example, i.e., a composite anatomical structure made of more than 10 tightly connected bones, which can be scrutinized altogether or separately. Morphological variations at different scales on the cranium may be influenced by multiple developmental processes acting in different and overlapping cranial regions (Hallgrímsson et al., 2009; Kyomen et al., 2023) and may be subject to different selective pressures and evolutionary processes (Mitteroecker et al., 2020). It is thus not surprising that a heterogeneous expression of allometry can be found among cranial subunits and on the entire cranium (Gonzalez et al., 2011; Le Verger et al., 2020). Searching for allometric variation at different anatomical scales on the cranium can also reveal local allometric shape changes that go unnoticed at the global scale. The consideration of different anatomical scales is thus critical to recovering a more complete picture of the complex allometric variation in composite structures.

The comparative study of allometry at different variational levels and anatomical scales is still a relatively unexplored research area (e.g., Chatterji et al., 2022; Cheverud, 1982a; Klingenberg, 2014; Klingenberg & Zimmermann, 1992; Klingenberg et al., 2012; Strelin et al., 2016; Urošević et al., 2013, 2018). We use this approach to reveal allometric shape changes expressed both within species and among lineages across the cranium of extant armadillos (order Cingulata). Cingulates are part of the Xenarthra, one of the four major clades of placental mammals (e.g., Zachos, 2020), and have two main advantages for investigating allometry in a comparative approach. First, the extant representatives of this clade span a wide range of body sizes, with weights ranging from approximately 100 g to over 50 kg (McDonough & Loughry, 2018; Superina & Abba, 2018). Second, cingulates exhibit substantial ontogenetic and evolutionary patterns of morphological variation relative to other mammalian clades, as evidenced by their considerable snout elongation (e.g., Hautier et al., 2017), and thus are a particularly relevant model clade for investigating cranial allometric shape changes. For the cranium, only a few studies have preliminarily assessed

evolutionary allometry (Abba et al., 2015; Cardini, 2019a; Feijó et al., 2018; Hautier et al., 2017; Machado et al., 2022; Moeller, 1968), without focusing on the shape deformations associated with size. An in-depth investigation of cranial allometry within nine-banded armadillos has shown great potential to improve our understanding of the ontogenetic and evolutionary dynamics of allometric shape changes (Le Verger et al., 2020). Using 3D GMM to characterize allometric patterns for the entire cranium and for its constitutive subunits, we propose to test the hypothesis that the allometric patterns detected in nine-banded armadillos are similar in two phylogenetically distant armadillo species. Second, we investigate whether such allometric patterns can be found at the evolutionary level in a dataset that includes nearly all the extant cingulate diversity.

Material and methods

Sampling

For our exploration of allometric variation at the static and ontogenetic levels, we sampled developmental series from juveniles to adult stages in two extant cingulate species belonging to the family Chlamyphoridae (Gibb et al., 2016), one euphractine and one tolpeutine, and compared them with that of a member of the family Dasypodidae, the nine-banded armadillo *Dasypus novemcinctus* Linnaeus, 1758 (Le Verger et al., 2020; Figure 1). For the Euphractinae, we sampled the extant *Zaedyus pichiy* Desmarest, 1804 ($n = 43$). According to the literature (Abba et al., 2015; Carlini et al., 2016; Superina & Abba, 2014), pichis can be mistaken for *Chaetophractus vellerosus* Gray, 1865 based on similar osteological features. We therefore assessed the taxonomical identification of our specimens using a statistical approach testing for the morphological homogeneity within the sample (see Supplementary Material S1). For the Tolpeutinae, we sampled a species complex ($n = 32$) consisting of *Cabassous unicinctus* Linnaeus, 1758 and *Cabassous centralis* Miller, 1899. Doubt exists about the distinction between these two species of *Cabassous* that are weakly differentiated morphologically and genetically (Feijó et al., 2021; Gibb et al., 2016; Hayssen, 2014; Wetzel, 1980, 1985). Our investigation of the cranial shape variation within our sample of *C. unicinctus* and *C. centralis* did not reveal significant differences (see Supplementary Material S2). For this reason, and for the overall weak morphological and molecular differentiation mentioned above, we used both species in the same dataset as a species Supplementary Material S2).

In the exploration of allometric variation at the evolutionary level, our sampling includes 21 extant species covering all extant armadillo genera and all but two extant species (Feijó et al., 2019, 2021; Gibb et al., 2016; *Dasypus beniensis* Lönnberg, 1942 and *Dasypus sabanicola* Mondolfi, 1968 are missing here). For *D. novemcinctus*, the Guianan morphotype, the Northern/Central morphotype, and the Southern morphotype, which are likely distinct species (Arteaga et al., 2020; Billet et al., 2017; Feijó et al., 2018, 2019; Gibb et al., 2016; Hautier et al., 2017; Huchon et al., 1999), were included bringing the total number of specimens sampled at the evolutionary level to $n = 23$, with one adult specimen per species to ensure homogeneous sampling. Sexual dimorphism in size in armadillos is only known in a few species, where it is generally low, generating much lower intraspecific size differences than interspecific ones (e.g., McDonough, 2000;

Silveira et al., 2009; Squarcia et al., 2009). The complete list of specimens is provided in [Supplementary Table S1](#). Additional information such as references and abbreviations are available in [Supplementary Material S3](#).

3D Reconstructions

Specimens were scanned at the X-ray microtomography imagery platforms of the American Museum of Natural History (New York, USA), the Royal Ontario Museum (Toronto, Canada), the Muséum national d'Histoire naturelle (Paris, France-AST-RX platform), the University of Montpellier (France-MRI platform), the Naturalis Biodiversity Center (Leiden, Netherlands), the Royal Belgian Institute of Natural Sciences (Brussels, Belgium), the Museum für Naturkunde (Berlin, Germany), and the State Museum of Natural History of Stuttgart (Germany). Three-dimensional reconstruction and visualization of the crania and cranial subunits were performed using image stacks with MIMICS v. 21.0 software (3D Medical Image Processing Software, Materialize, Leuven, Belgium), as in [Le Verger et al. \(2020\)](#). Image stacks were improved in contrast, rotated, cropped, and reduced to 8 bits using the ImageJ software ([Schneider et al., 2012](#)).

Geometric morphometrics

Cranial shapes were quantified with 114 anatomical landmarks ([Supplementary Figure S1](#), [Supplementary Tables S2](#) and [S3](#)) placed on the exported 3D models using AVIZO v. 9.7.0 software (Visualization Sciences Group, Burlington, MA, USA). In comparison with the previous study on nine-banded armadillos, 17 landmarks were removed from the original dataset ([Le Verger et al., 2020](#)), since they could not be placed on the crania of *Zaedyus* and *Cabassous* (homologous structures were absent or not observable). The remaining 114 landmarks were initially used for the analyses of the *Dasybus novemcinctus* complex ([Le Verger et al., 2020](#); [Supplementary Table S2](#)). None of the previously defined cranial subunits, initially called Operational Bone Units, included less than four landmarks after the reduction of the landmark dataset, thus keeping all cranial subunits available for analyses ([Le Verger et al., 2020](#)). Because the analysis was already conducted on a larger dataset both in terms of number of specimens ($n = 76$) and landmarks ($n = 131$), we refer in the present work to the most robust statistical results obtained for *Dasybus novemcinctus* in [Le Verger et al. \(2020\)](#). However, to facilitate comparisons, here, all visualizations of widespread allometric variations correspond to a re-analysis of the Southern morphotype of *Dasybus novemcinctus* ($n = 48$), corresponding to the reduced landmark set of the present study after checking the similarity of deformations between the Southern morphotype and the total dataset (see [Le Verger et al., 2020](#)), and between the reduced and extended landmark datasets.

For all pre-analysis treatments, we followed the approach of [Le Verger et al. \(2020\)](#). We performed a generalized Procrustes analysis ([Rohlf & Slice, 1990](#)) using the function *gpagen* in the R package *geomorph* version 4.0.4 ([Adams et al., 2022](#)). Intra-individual asymmetries ([Klingenberg et al., 2002](#)) were removed using the function *symmetrize* in the R package *Morpho* version 2.6 ([Schlager, 2017](#)). When some landmarks were missing on one side of the cranium, their position was estimated using the function *fixLMmirror* in the *Morpho* R package (this represented less than 4% of the intraspecific datasets and less than 3% of the interspecific datasets—[Supplementary Table S4](#)). Missing landmarks on

the cranial midline or landmarks missing on both sides were estimated in intraspecific datasets with the function *estimate.missing* in the R package *geomorph* (0.8% of the dataset; [Supplementary Table S4](#)).

Ontogenetic stages determination

For each intraspecific dataset within *Cabassous* and *Zaedyus*, we subdivided the sample into different ontogenetic stages in order to study allometric patterns at the ontogenetic and static levels ([Le Verger et al., 2020](#)). For nine-banded armadillos, three ontogenetic stages were previously recognized—juvenile, subadult, and adult—based on three variables: dental eruption, cranial ossification, and total cranial length ([Le Verger et al., 2020](#)). Because *Cabassous* and *Zaedyus* only have one dental generation, in contrast to *Dasybus* ([Ciancio et al., 2012](#)), dental eruption could not be used to determine ontogenetic stages as in [Le Verger et al. \(2020\)](#). For these taxa, we used the basicranial ossification degree following the criteria of [Hubbe et al. \(2016\)](#), which include the same three genera, and were considered as adults those specimens in which the supraoccipital-exoccipital, basioccipital-basisphenoid, and basioccipital-exoccipital contacts are completely closed (bones fused). Conversely, a specimen with completely unfused supraoccipital-exoccipital contact was considered as a juvenile and specimens with intermediate degrees of ossification for these three sutures were attributed to the subadult stage. The ontogenetic stages determination in *Zaedyus* and *Cabassous* is less distinct than in *Dasybus*, although we still tend to obtain an ontogenetic continuum from juveniles to adults, with more overlap among stages in *Cabassous* ([Supplementary Materials S1 and S2](#); [Le Verger et al., 2020](#); see [Discussion](#)). Based on these criteria, our sampling for the ontogenetic level encompassed all specimens for the three ontogenetic stages (*Zaedyus* $n = 43$; *Cabassous* $n = 32$) whereas analyses at the static level included only adult specimens (*Zaedyus* $n = 23$; *Cabassous* $n = 22$). A complete account of the observations for these criteria and attributions to ontogenetic stages for each specimen can be found in [Supplementary Table S5](#) (see [Supplementary Materials S1 and S2](#) for more details and [Supplementary Figure S2](#) for an illustration of each ontogenetic stage for each developmental series).

Phylogenetic considerations

For the analyses at the evolutionary level, the phylogenetic relationships of taxa must be considered ([Felsenstein, 1985](#); [Klingenberg & Marugán-Lobón, 2013](#)). We used the time-tree of [Gibb et al. \(2016\)](#), which includes all extant species of armadillos. Slight modifications were made to this tree for the dasypodines in order to incorporate some changes from the recent reassessment of their phylogeny and taxonomic diversity ([Feijó et al., 2019](#); [Figure 1](#)). The reconstructed phylogenetic tree is illustrated in [Figure 1](#).

Allometric analyses and detection of widespread variations

To quantify the covariance between cranial shape and size, we used the same approach as [Le Verger et al. \(2020\)](#), including two anatomical scales: the entire cranium and cranial subunits—called respectively “entire skull” and “bone-by-bone” in this previous study. We used the same specimens for both approaches. While the entire cranium Procrustes alignment was realized on the entire set of cranial landmarks,

each cranial subunit Procrustes alignment was realized on a reduced set of landmarks corresponding to the cranial subunit under consideration, with a slight difference in the number of landmarks compared to [Le Verger et al. \(2020\)](#) (see [Supplementary Table S6](#)). A separate Procrustes alignment for each cranial subunit was adopted rather than subdividing the Procrustes alignment of the entire cranium. This strategy was selected to explore the anatomical extent of allometric variations—entire cranium and/or cranial subunits—helping to determine whether the detected shape changes were expressed globally and/or locally on the cranium. The cranium is subjected to multiple processes acting regionally, local allometric variations presumably exist beyond global ones. Using separate superimpositions at various anatomical scales represents an efficient means to detect both global and local trends, thus preventing allometric variation detected on a global scale from masking more localized allometric variations ([Le Verger et al., 2020](#)). This approach also served to detect allometric shape changes expressed at several anatomical scales, affecting cranial structures both globally and locally (e.g., postorbital constriction—see *Results*). Finally, carrying out shape analyses at these two anatomical scales may also help filter out minor scale-specific biases potentially induced by Procrustes analyses on patterns of shape and size covariation ([Cardini, 2019b](#)). We performed the cranial subunit analyses only on the left side of the cranium, which was more complete in most cases. The allometric component of shape variation for cranial subunits and for the entire cranium was analyzed using the logarithm of the centroid size of the cranium as a measure of size ([Monteiro, 1999](#)). For intraspecific datasets, for both the entire cranium and cranial subunit analyses of allometry, we performed a multivariate regression of Procrustes shape coordinates on the log centroid size ([Monteiro, 1999](#)), with a randomization of residuals in permutation procedures (iterations = 10,000) using the function *procD.lm* of the R package *geomorph*. For the evolutionary level, we performed a phylogenetic regression under a Brownian motion model of evolution (phylogenetic generalized least squares using our baseline tree—[Adams & Collyer, 2018](#); [Klingenberg & Marugán-Lobón, 2013](#); [Rohlf, 2001](#)) for Procrustes shape variables on the log centroid size using the function *procD.pgls* of the R package *geomorph*. We used the same statistical approach as for nine-banded armadillos ([Le Verger et al., 2020](#)) to analyze the intraspecific and evolutionary datasets. For graphical display, we used the projected regression scores of the shape data to represent shape variation related to changes in log centroid size ([Adams et al., 2013](#)). Shape changes are visualized as vectors from the minimal shape (blue) to the maximal shape (gold) of the shape regression scores corresponding to the projection of the data points in shape space onto an axis in the direction of the regression vector (see [Drake & Klingenberg, 2008](#)). The extraction of widespread allometric variations corresponds to the interpretation of the displacement of one or more landmarks with respect to the displacement of the whole landmark conformation for a given structure (i.e., entire cranium or cranial subunit). For each multivariate regression, the coefficients of determination R^2 indicated the proportion of shape variation accounted for by size variation (hereafter called allometric proportion) according to a linear model.

We focus on the widespread allometric variations, i.e., the similar allometric shape changes detected across the three variational levels for each anatomical scale. These are selected

using the following criteria for the cranium or a given cranial subunit: (a) allometric variation is significant at least at the ontogenetic level in all datasets and at the evolutionary level; (b) part of the allometric shape change is similar at least at the ontogenetic levels in all datasets and at the evolutionary level; and (c) allometric proportions of shape variation (R^2) are relatively high compared to other cranial subunits (NB: allometric signal has been scrutinized for the Z -scores as well). The criterion (b) corresponds to the comparative observation of the set of vectors extracted from the multivariate regression of each dataset. A given allometric shape change is deemed similar across datasets when the vectors in each dataset involve the relative displacement of the same landmark(s) in the same direction compared to the whole conformation. For (c), the allometric proportions of each cranial subunit are compared across all levels and assigned a relative score that serves as a summary evaluation of their allometric signal across datasets relative to other cranial elements. For a given dataset and level of variation, the scores assigned to the 13 cranial subunits range from 13 (highest) to 1 (lowest). When two cranial subunits have the same R^2 value, then they get attributed the same score and the next lower score is not attributed. If the allometry is not statistically detected for a cranial subunit (i.e., p -value > .05) then its score is 0. The final score of a given cranial subunit is obtained by summing its scores for each dataset at each level of variation (see [Supplementary Table S7](#)). Here, the ranking is used as a visualization tool and only serves to summarize the results. For each analysis, we provide the full set of related metrics ([Supplementary Table S8](#)).

Comparison of allometric trajectories

Differences in allometric trajectories among developmental series of different species or among clades (“subfamilies”/families) were investigated to detect whether different allometric trends exist at these variational levels. For these analyses, we tested whether the allometric trajectories are significantly different among the developmental series of different species at the static and ontogenetic levels. At the evolutionary level, we also tested whether the allometric trajectories are significantly different among the four “subfamilies” (Dasypodinae, Euphractinae, Chlamyphorinae, and Tolypeutinae) and the two families (Dasypodidae and Chlamyphoridae) of Cingulata ([Delsuc et al., 2016](#)). Because sampling at the “subfamilial” level is particularly low for some “subfamilies” ($N < 5$), we mainly interpret results for the familial level, while presenting the “subfamilial” level as an indication only, calling for caution. For each analysis, we defined one model for different allometric trajectories (shape ~ centroid size * taxa) and one model for common allometric trajectories (shape ~ centroid size + taxa) and compared these two allometric models using an analysis of variance (ANOVA). The appropriate allometric model is thus selected and plotted using the *plotAllometry* function of the *geomorph* package in R. This approach is similar to a homogeneity of slope test using a Procrustes ANOVA ([Goodall, 1991](#)) and follows the recommendation given with the *geomorph* package in R ([Adams et al., 2022](#); [Baken et al., 2021](#); [Collyer & Adams, 2018, 2021](#)). This approach gives an overall statistical assessment of the difference in allometric slope between two or more groups and thus serves as a way to summarize the results of allometric trajectory comparisons. Complementarily, we have performed pairwise comparisons between allometries to assess the angle between each slope

and the differences in the total length of allometric vectors between each group, providing the upper confidence interval in each case. A more exhaustive description of the approach is available in [Zelditch and Swiderski \(2022\)](#). This last step was performed using the *pairwise* function of the *RRPP* R package ([Collyer & Adams, 2018](#)).

Allometric space

We synthetically represented the diversity of allometric patterns at a given anatomical scale and for the various variational levels (ontogenetic, static, and evolutionary) using the allometric space approach (see [Gerber et al., 2008](#), and [Gerber & Hopkins, 2011](#) for geometric morphometric data). To do so, we aligned, symmetrized, and extracted size and shape data for all specimens in a single analysis (unique generalized Procrustes analysis). We then used various partitions of the shape and size data to characterize allometric patterns at the ontogenetic and static levels for *Dasyopus*, *Zaedyus*, and *Cabassous*, and at the evolutionary levels for the clades Cingulata, Dasypodidae, and Chlamyphoridae (some individuals were thus assigned to several partitions). Allometric patterns were captured by the slope coefficients obtained from multivariate linear regressions of shape on size for the relevant partitions of the data. A given allometric pattern was therefore depicted as a point in allometric space and we also plotted the isometric pattern (a vector of zero slope coefficients) as a reference to assess the degree of allometry of the various allometric patterns. The farther the point of a variational level for a given dataset is from the isometric referential (the greater the deviation from isometry), the greater the shape change for a given size change. Confidence ellipses for the allometric pattern estimates were obtained by bootstrap resampling (250 replicates), providing an assessment of the mean allometric pattern estimates and their confidence intervals. The analyses were carried out in R ([R Core Team, 2021](#); script in [Supplementary Material S4](#)) and followed the protocol defined by [Gerber and Hopkins \(2011\)](#).

Results

Allometric trajectories at different variational levels

When each dataset was taken separately, allometric variation was detected in the majority of anatomical scales and variational levels analyzed ([Supplementary Table S8](#)). When analyzed jointly, different allometric trajectories are detected for the three developmental series at all anatomical scales, i.e., for the entire cranium, as well as for each cranial subunit ([Figure 2A](#), [Supplementary Figure S3](#), [Table 1](#)). At the evolutionary level, differences among allometric trajectories of families are generally not significantly supported at p -values $< .05$, except for a few cranial subunits (frontal, squamosal, sphenopterygoid complex (as-os-pt-bs), and basioccipital-exoccipital complex (bo-eo); [Table 1](#)). However, p -values are just a little higher than this threshold for the entire cranium, premaxillary, maxillary, jugal, and parietal ([Supplementary Figure S3](#), [Table 1](#)), meaning that different allometric trajectories among families are not far from being supported for these cranial units as well. Analyses of the angles between allometric slopes and total allometric vector lengths deliver partly similar results, with trajectories among ontogenetic or static series being most often statistically different, while differences among evolutionary trajectories are far from being significant to the exception of the entire cranium ([Supplementary Table](#)

[S9](#)). Furthermore, these analyses allow us to detect fewer differences in allometric trajectories between *Cabassous* and *Zaedyus* than between those two genera and *Dasyopus* at intraspecific levels ([Supplementary Table S9](#)). The results obtained at the “subfamilies” level are similar to those at the family level, except that no different allometric trajectories are detected ([Table 1](#) and [Supplementary Table S9](#)).

Widespread allometric variations at the entire cranial scale

At the ontogenetic level, allometry explains a higher proportion of shape variation of the entire cranium in *Dasyopus* than in *Zaedyus* and *Cabassous*, while *Zaedyus* and *Cabassous* show a higher allometric proportion than *Dasyopus* at the static level ([Supplementary Table S8](#), [Figures 2](#) and [3](#)). Even removing the youngest specimens for *Dasyopus*, the highest allometric proportion is still found in this genus (without the youngest: $R^2 = 17\%$, p -value $< .0001$; without the two youngest: $R^2 = 13\%$, p -value $< .0001$). *Zaedyus* and *Cabassous* also show a higher allometric proportion at the static level than at the ontogenetic level, which contrasts with *Dasyopus*. Despite significantly different allometric trajectories among these species, many shape changes accompanying an increase in cranial size were comparable across the three intraspecific series and were also found at the evolutionary level ([Figure 2C](#) and [D](#); [Supplementary Figure S3](#)). When size increases, in all datasets and at all variational levels, the most common allometric variations are a relative flattening of the cranial roof and a strong reduction of the braincase proportions ([Figure 2C](#) and [D](#)). These are accompanied by a stronger postorbital constriction, a relative widening of the temporal fossa, and a relatively more salient nuchal crest process posteriorly ([Figure 2C](#) and [D](#)). Anteriorly a strong relative elongation of the snout with increasing size ([Figure 2C](#) and [D](#)) was also found for all datasets.

The shape differences between small and large adult individuals (static allometries) are similar—though less pronounced—than those observed between juvenile and adult specimens in the developmental series (ontogenetic allometries), especially in *Dasyopus* ([Figure 2C](#) and [Supplementary Figure S3](#)). Conversely, at the evolutionary level, the shape differences between small and large species are more prominent than those observed between small and large specimens at the intraspecific level ([Figure 2C](#)). Finally, the dasypodids exhibit several allometric shape changes that depart from those of chlamyphorids ([Figures 1](#) and [2](#) and [Supplementary Figure S3](#)), such as the convergence of the nuchal crests towards the midline or the relative retention of snout width as size increases. Additional information regarding each plot at all variational levels and the illustrations of allometric variations at the static level are available in [Supplementary Figure S3](#).

Distribution of allometry at the cranial subunit scale

Investigation at the cranial subunit scale highlights a heterogeneous distribution of shape changes correlated to size across cranial subunits and a strong dissimilarity of these distributions across levels and datasets ([Figure 3](#) and [Supplementary Table S8](#)). Several cranial subunits do not show significant allometric variation, particularly at the static level ([Figure 3A](#)). Comparison of the intraspecific series and the evolutionary level reveals that the frontal and petrosal are systematically affected by allometry, with high proportions for the

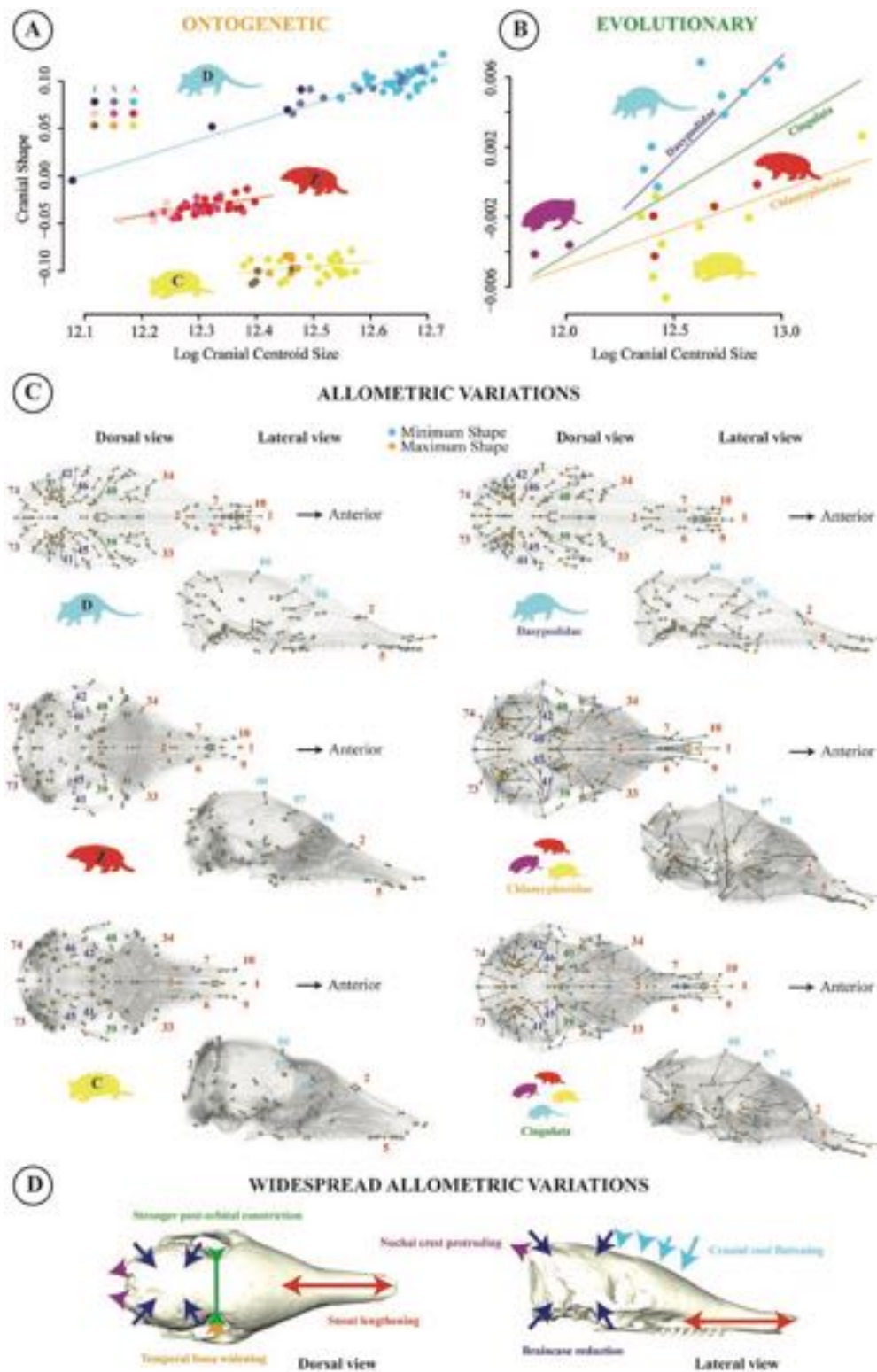


Figure 2. Allometric patterns at the entire cranial scale. (A) Multivariate regression performed for the comparison of allometric trajectories among the three developmental series at the ontogenetic level. (B) Multivariate regression of shape on size at the evolutionary level. (C) Allometric variations detected at the ontogenetic (left) and evolutionary (right) levels in each dataset. In order to facilitate the identification of widespread allometric variations discussed in the text, we have colored corresponding landmark numbers (Supplementary Table S2). (D) Diagrammatic summary of the widespread allometric variations using the same colors as in (C) (see text). Results for the static level are presented in Supplementary Figure S3. The statistical results of the ANOVAs with permutational tests are presented in Table 1 and Supplementary Tables S8 and S9. Abbreviations: A, adult; C, *Cabassous* spp.; D, *Dasyproctidae* Southern Morphotype; J, juvenile; S, subadult; Z, *Zaedyus pichiy*.

Table 1. Statistical results for the allometric slope comparisons at the intraspecific and interspecific (i.e., among “subfamilies” and families) levels. A significant p -value ($< .05$) means that the hypothesis of a different allometry is supported. Significant p -value ($< .05$) are in bold.

Intraspecific slope comparison																	
Ontogenetic level																	
N	ResDf	RSS	SS	MS	R ²	F	Z	P	N	ResDf	RSS	SS	MS	R ²	F	Z	P
Cranium	123	119	0.3397	0.2747	0.2747	0.1792	3.0583	0.001	78	74	0.1742	0.2197	0.2197	0.2197	93.317	3.1535	0.001
Premax.	123	119	2.2232	1.3007	1.3007	0.2233	4.6172	0.001	78	74	1.1694	1.1754	1.1754	1.1754	74.378	4.7740	0.001
Maxillary	123	119	1.0100	0.9131	0.9131	0.2303	3.5485	0.001	78	74	0.5088	0.7905	0.7905	0.7905	114.97	3.6565	0.001
Nasal	123	119	0.5038	0.0854	0.0854	0.0501	5.0347	0.001	78	74	0.2554	0.0657	0.0657	0.0657	19.043	4.7668	0.001
Frontal	123	119	0.8984	0.6414	0.6414	0.2855	4.0249	0.001	78	74	0.4727	0.5243	0.5243	0.5243	82.079	3.7995	0.001
Lacrimal	123	119	2.4741	0.6665	0.6665	0.1405	5.2926	0.001	78	74	1.4058	0.6352	0.6352	0.6352	33.435	5.4702	0.001
Jugal	123	119	1.2107	0.5174	0.5174	0.1453	6.4339	0.001	78	74	0.7341	0.3629	0.3629	0.3629	36.577	6.0440	0.001
Palatine	123	119	1.2510	0.4604	0.4604	0.0395	43.791	0.001	78	74	0.8316	0.2958	0.2958	0.2958	26.321	6.2709	0.001
Parietal	123	119	0.7353	0.2630	0.2630	0.1215	5.5697	0.001	78	74	0.4092	0.2276	0.2276	0.2276	41.158	5.4683	0.001
Squamosal	123	119	1.3701	0.6194	0.6194	0.1487	4.892	0.001	78	74	0.7873	0.4809	0.4809	0.4809	45.198	4.1531	0.001
As-Os-Pr-Bs	123	119	1.5814	0.3084	0.3084	0.0706	7.6854	0.001	78	74	0.9250	0.2322	0.2322	0.2322	18.576	6.2878	0.001
Supraocc.	123	119	1.3905	0.2608	0.2608	0.0781	7.0483	0.001	78	74	0.7998	0.2142	0.2142	0.2142	10.64	19.817	0.001
Bo-Eo	123	119	0.6612	0.1405	0.1405	0.1297	5.6828	0.001	78	74	0.3895	0.1227	0.1227	0.1227	23.318	5.6638	0.001
Petrossal	123	119	1.2700	0.3863	0.3863	0.1011	36.205	0.001	78	74	0.7180	0.3687	0.3687	0.3687	37.999	4.6768	0.001

Interspecific slope comparison																	
“Subfamilial” level																	
N	ResDf	RSS	SS	MS	R ²	F	Z	P	N	ResDf	RSS	SS	MS	R ²	F	Z	P
Cranium	23	22	0.0250	0.0078	0.0078	0.1853	0.9074	0.1928	23	22	0.0308	0.0035	0.0035	0.0035	2.1393	1.3856	0.0855
Premax.	23	22	0.0998	0.0285	0.0285	0.2038	0.7290	0.2361	23	22	0.1134	0.0174	0.0174	0.0174	2.9215	1.5967	0.0619
Maxillary	23	22	0.0443	0.0110	0.0110	0.1577	0.5716	0.2793	23	22	0.0520	0.0057	0.0057	0.0057	2.0839	1.4504	0.0789
Nasal	23	22	0.0280	0.0049	0.0049	0.1196	-0.0763	0.5271	23	22	0.0337	0.0020	0.0020	0.0020	0.0500	1.1515	0.3298
Frontal	23	22	0.0304	0.0100	0.0100	0.1687	1.1583	0.1296	23	22	0.0362	0.0072	0.0072	0.0072	0.1206	3.7570	0.0054
Lacrimal	23	22	0.1892	0.0136	0.0136	0.0549	-1.4600	0.9272	23	22	0.2063	0.0061	0.0061	0.0061	0.0245	0.5584	0.6271
Jugal	23	22	0.0987	0.0193	0.0193	0.1340	0.9762	0.0662	23	22	0.1085	0.0139	0.0139	0.0139	0.0966	2.4351	0.0763
Palatine	23	22	0.0731	0.0097	0.0097	0.0852	-0.6092	0.7251	23	22	0.0839	0.0047	0.0047	0.0047	0.0414	1.0695	0.3777
Parietal	23	22	0.0363	0.0153	0.0153	0.2443	1.2321	0.1192	23	22	0.0454	0.0069	0.0069	0.0069	0.1102	2.8895	0.0654
Squamosal	23	22	0.1207	0.0412	0.0412	0.2226	1.7056	0.9801	23	22	0.1429	0.0226	0.0226	0.0226	0.1223	3.0073	0.0495
As-Os-Pr-Bs	23	22	0.1700	0.0686	0.0686	0.2466	2.0166	1.2397	23	22	0.2053	0.0387	0.0387	0.0387	0.1393	3.5845	0.0334
Supraocc.	23	22	0.0964	0.0315	0.0315	0.2170	1.6360	0.9576	23	22	0.1183	0.0122	0.0122	0.0122	0.0839	1.9596	0.1120
Bo-Eo	23	22	0.0506	0.0184	0.0184	0.2325	1.8188	1.0361	23	22	0.0568	0.0133	0.0133	0.0133	0.1681	4.4513	0.0166
Petrossal	23	22	0.1153	0.0309	0.0309	0.1795	1.3378	0.6258	23	22	0.1355	0.0143	0.0143	0.0143	0.0834	2.0080	0.1115

Note. As = alisphenoid; ResDf = degrees of freedom; *bo* = basioccipital; *bs* = basisphenoid; *eo* = exoccipital; F = Fisher-test; MS = mean squares; N = total number of individuals; os = orbitosphenoid; P = p-value, significance following the permutation test; Premax. = Premaxillary; pr = prerygoid; R² = proportion of the variance for a dependent variable (here, cranial shape) that's explained by an independent variable (here, size) in a linear model; RSS = residual sum of squares; SS = sum of squares; Supraocc. = Supraoccipital; Z = z-score.

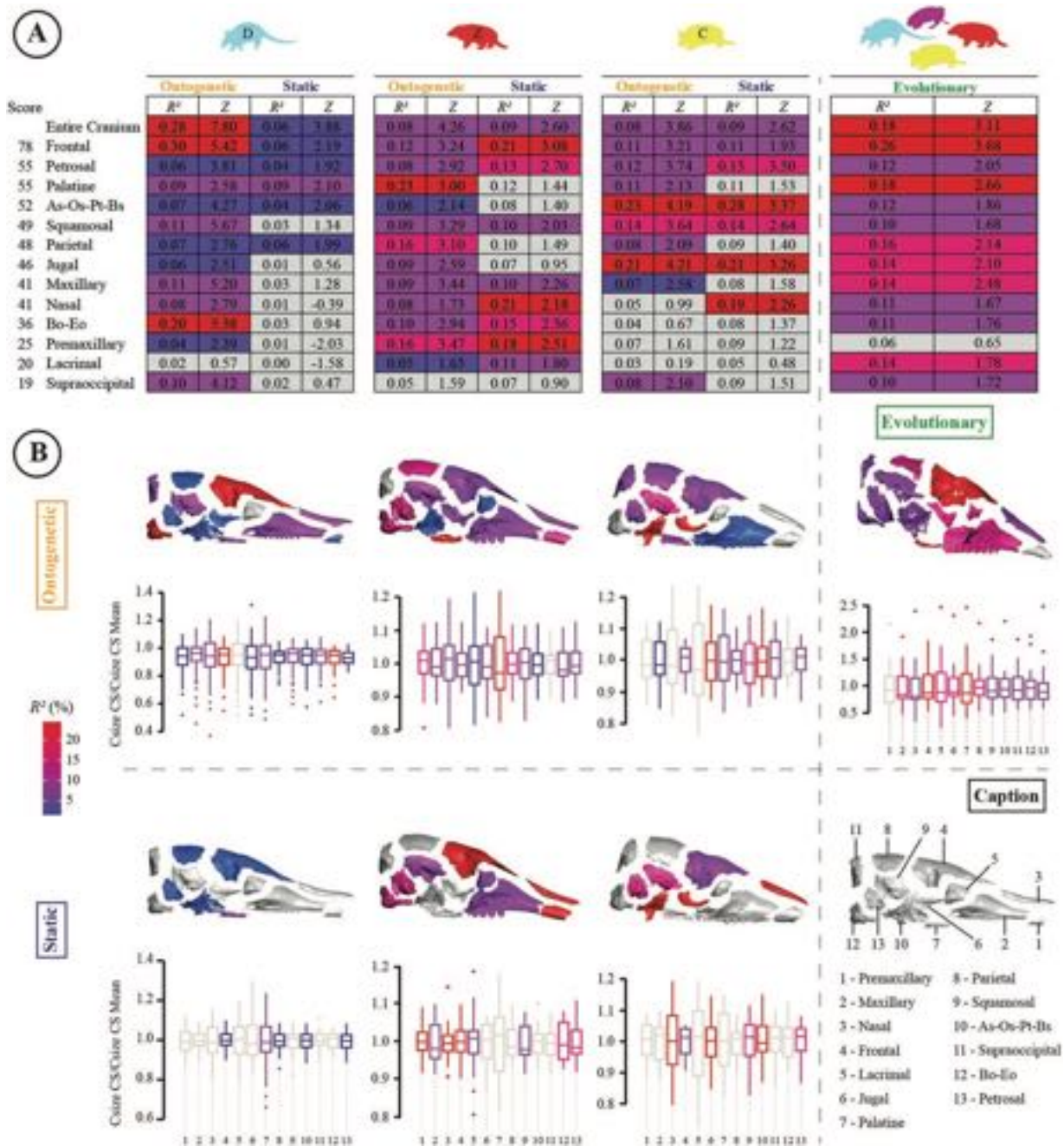


Figure 3. Distribution of cranial allometry and size variation across cranial subunits. (A) Allometric proportions of shape variation across the cranium (entire cranium and cranial subunit). The tables gather the set of coefficients of determination ($=R^2$) and Z-scores ($=Z$) from each multivariate regression. Each table cell, and boxplot were colored according to the R^2 value. Absence of color implies a non-significance of the statistical test (p -value $> .05$). Scores reported on the left reflect a ranking of the allometric signal of each cranial subunit based on the comparison of their allometric proportions at each level of variation (see [Supplementary Table S7](#)). (B) Boxplots showing the variation in size (log centroid size) for each cranial subunit relative to its mean in each dataset (ontogenetic, static, and evolutionary levels). Associated allometric proportions are reported in corresponding colors on virtually dislocated crania (in right lateral view). Additional information is available in [Supplementary Tables S7 and S8](#) and [Supplementary Figures S8–S12](#). Abbreviations: as, alisphenoid; bo, basioccipital; bs, basisphenoid; C, *Cabassous* spp.; CS, cranial subunit; D, *Dasybus*; eo, exoccipital; os, orbitosphenoid; pt, pterygoid; Z, *Zaedyus*.

former (Figure 3A). The shapes of the squamosal and sphenopterygoid complex (i.e., as-os-pt-bs) are also affected by allometry, except at the static level in *Dasybus* and *Zaedyus*, respectively (Figure 3A and B). Finally, the palatine, parietal, jugal, and maxillary show more variable allometric proportions among series at the static level while the remaining cranial subunits are variable at all intraspecific levels (Figure 3B).

The variation in size of each cranial subunit at each level for each dataset is variable and does not appear to correlate

with the amount of allometric proportion in their shape variation. The cranial subunits of the face tend to show a higher variation in size (Figure 3B). As explained in the *Material and methods* section, we compared the allometric proportions of each cranial subunit across all levels and assigned them a relative score. This resulted in the frontal being by far the cranial subunit with the strongest allometric signal across levels, followed by the petrosal and palatine bones ([Supplementary Table S7](#) and [Figure 3A](#)). When using the Z-scores, the frontal

remains the cranial subunit with the strongest allometric signal across levels, followed by the petrosal and the sphenopterygoid complex (Supplementary Table S7).

Widespread allometric variations at the cranial subunit scale

Following our selection criteria for a given cranial subunit (see *Material and methods* section “Allometric analyses and detection of widespread variations”), we detected allometric variations that were widespread across datasets for four cranial bones. These variations are briefly described below, in the case of an increasing cranial size. More information and details are shown in the Supplementary Data (Supplementary Figures S4–S14, Supplementary Tables S7–S10, and Supplementary Information S5). Apart from widespread allometric shape changes, variations unique to a given dataset were found for many cranial units as well.

Maxillary—As cranial size increases, the maxillary tends to display a reduced relative height (Figure 4).

Frontal—The frontal shows an increase in its thickness posteroventrally and a stronger postorbital constriction (Figure 4).

Squamosal—The squamosal exhibits a broader contact with the jugal on the zygomatic arch and a greater protrusion of the most posterior part of the zygomatic arch (Figure 4).

Petrosal—The petrosal exhibits a more ventrally protruding mastoid process and a shallower fossa subarcuata (Figure 4).

Allometric space across variational levels

The allometric space reveals contrasted patterns of allometric slope coefficients (Figure 5). For both the entire cranial scale and the cranial subunits, the static allometry of each series tends to be close to ontogenetic allometry, and *Dasypus* patterns are always closer to datasets at the evolutionary level than those of *Cabassous* and *Zaedyus* (Figure 5), except for the entire cranium scale where the Chlamyphoridae dataset overlaps with the *Cabassous* ones. Allometry in armadillos is manifested differently between the global (entire cranium) and local (cranial subunit) anatomical scales. For the entire cranium, *Dasypus* and the datasets at the evolutionary level correspond to the strongest deviations from the isometric reference (Figure 5A). For the cranial subunits, the trend is reversed with *Zaedyus* and *Cabassous* representing the most distant points from the isometric reference while *Dasypus* and the datasets at the evolutionary level are closer (Figure 5B–E). It is also noteworthy that the size of the confidence ellipses is quite unbalanced in analyses of cranial subunits: *Zaedyus* and *Cabassous* exhibit large ellipses while *Dasypus* and evolutionary datasets most often have distinctly smaller ellipses, meaning that their slopes are better characterized.

Discussion

Cranial allometry in Cingulates: distribution, widespread variations, and biological interpretations

Allometric patterns are expressed in a contrasted manner across multiple variational levels and anatomical scales, according to our results. The most widespread allometric

variation identified here corresponds to a relative lengthening of the snout associated with a relative reduction of the braincase proportions in large-sized specimens/species. This shape change, named CRaniofacial Evolutionary Allometry (= CREA), is well-known in a multitude of mammalian clades as well as some other vertebrates (Cardini, 2019a; Cardini et al., 2015; Cardini & Polly, 2013; Gould, 1975; Marcy et al., 2020; Osborn, 1912; Radinsky, 1982; Radinsky, 1984a, 1984b; Radinsky, 1985; Robb, 1935a, 1935b; Tamagnini et al., 2017; Weidenreich, 1941). In cingulates, CREA is a pervasive morphological trend, but it is not the only one. CREA is accompanied by other widespread allometric shape changes distributed over different regions of the cranium (Figure 4), some of which appear to potentially involve muscle-bone interactions and/or cranial growth constraints. The allometric variation of the petrosal bone illustrates both cases. As for many bony processes, the mastoid process of the petrosal in armadillos serves as a muscular attachment; here, the digastric muscle is involved in mandibular movement (Wible & Gaudin, 2004). A more protruding process may provide a proportionally larger attachment area for a potentially larger muscle. Another instance on the petrosal bone involves the relative reduction of the fossa subarcuata, which accommodates part of the cerebellum, with increasing cranial size. Because this fossa is usually circumscribed by the anterior semicircular canal of the inner ear, Billet et al. (2015) have questioned whether the reduced size of this canal in large taxa, in comparison to the petrosal, could constrain the shape of the fossa subarcuata. The allometric shape change detected here supports this hypothesis since large armadillos tend to show a shallower fossa subarcuata. Further anatomical interpretations of the detected widespread allometric shape changes are discussed in Supplementary Material S6.

The discovery of these widespread allometric variations may have important implications for morphological phylogenetics. Fluctuation in size may indeed systematically generate similar suites of allometric shape changes, convergently evolved in distantly related large-sized taxa. Since biological dependencies among traits represent a major challenge for morphological phylogenetics (e.g., Billet & Bardin, 2019; Goswami et al., 2014; Phillips et al., 2023), the detection of multiple cranial variations dependent on size emphasizes the need to account for allometry when building morphological matrices and designing character models.

Besides these widespread variations, we showed that cingulates exhibit varying strengths, or degree, of allometric variation (i.e., heterogeneous allometric proportions of shape variation) at different anatomical scales and variational levels. At the intraspecific level and entire cranial scale, *Dasypus* shows a much stronger ontogenetic allometry than static allometry, as commonly seen in mammals (Frost et al., 2003; Hallgrímsson et al., 2009, 2015). By contrast, *Zaedyus* and *Cabassous* show more similar allometric strengths between ontogenetic and static levels. Although defining ontogenetic stages proved to be more challenging for the latter (see Supplementary Materials 1 and 2, and Le Verger et al., 2020), dissimilarities among armadillo species may originate from different growth patterns (Porto et al., 2013). In mammals and birds, growth strategies associated with differential growth rates during ontogeny range from altriciality to precociality, the former defining a species whose offspring is open-eyed from birth in contrast to the latter (Isler & van Schaik, 2009). *Dasypus* is precocial while *Zaedyus* and *Cabassous*

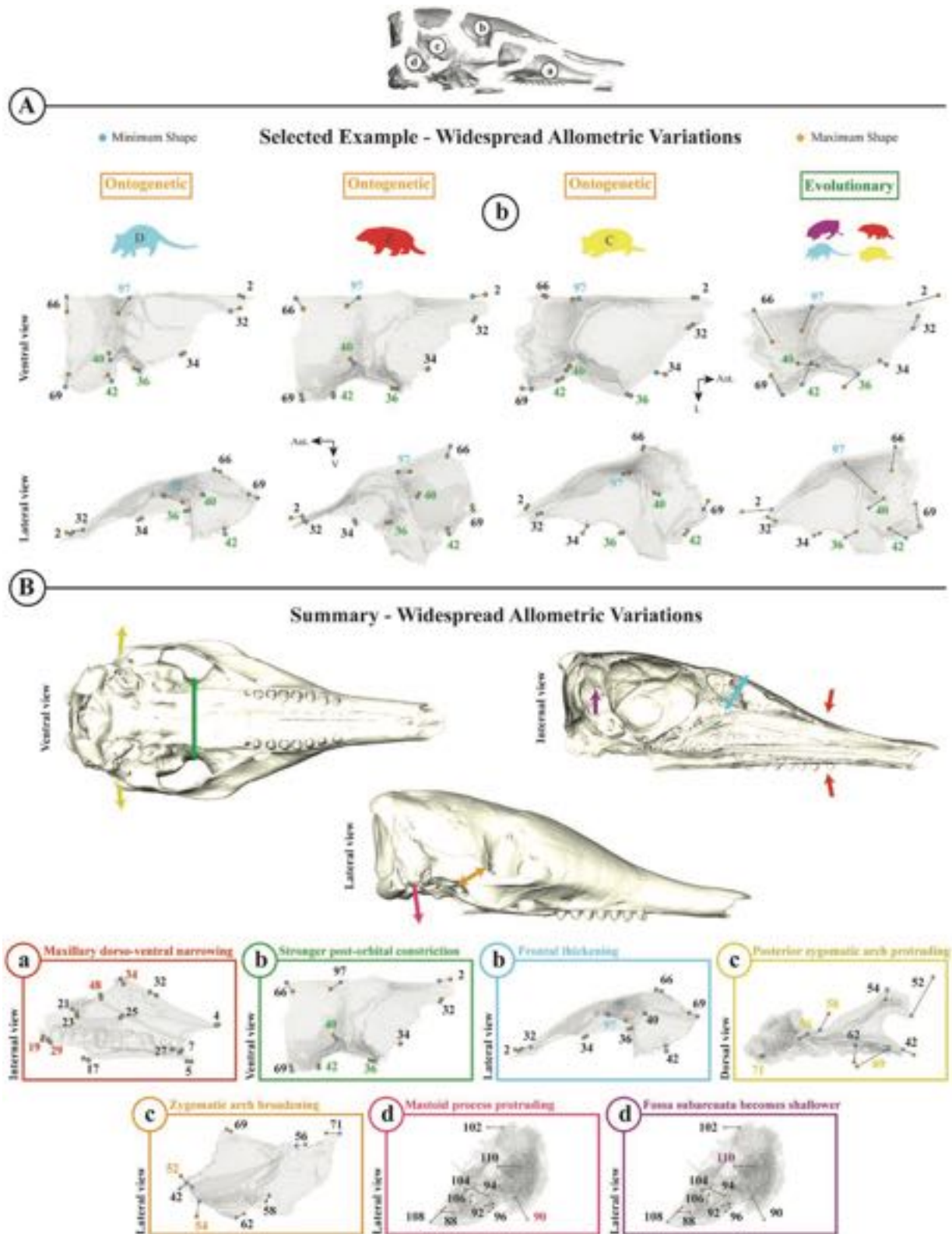


Figure 4. Selection protocol and diagrammatic summary of the widespread allometric variations at the cranial subunit scale detected at the ontogenetic and evolutionary levels in each dataset. Lower-case letters refer to the cranial subunit illustrated in the dislocated skull. (A) Selected example on the frontal (b) with colored landmarks depicting a widespread allometric variation in relation to the overall landmark conformation (Supplementary Table S2). (B) Diagrammatic summary of widespread allometric variations on a cranium in different views. For each widespread allometric variation, a vignette illustrating the concerned cranial subunit accompanies the summary. Detailed illustrations supporting the detection of widespread allometric variations are available in Supplementary Figures S4 and S5. More details are provided in Supplementary Material S5, Supplementary Figures S4–S14, Table 1, and Supplementary Tables S7–S9. Abbreviations: Ant., anterior; C, *Cabassous* spp.; D, *Dasybus*; L, lateral; V, ventral; Z, *Zaedyus*.

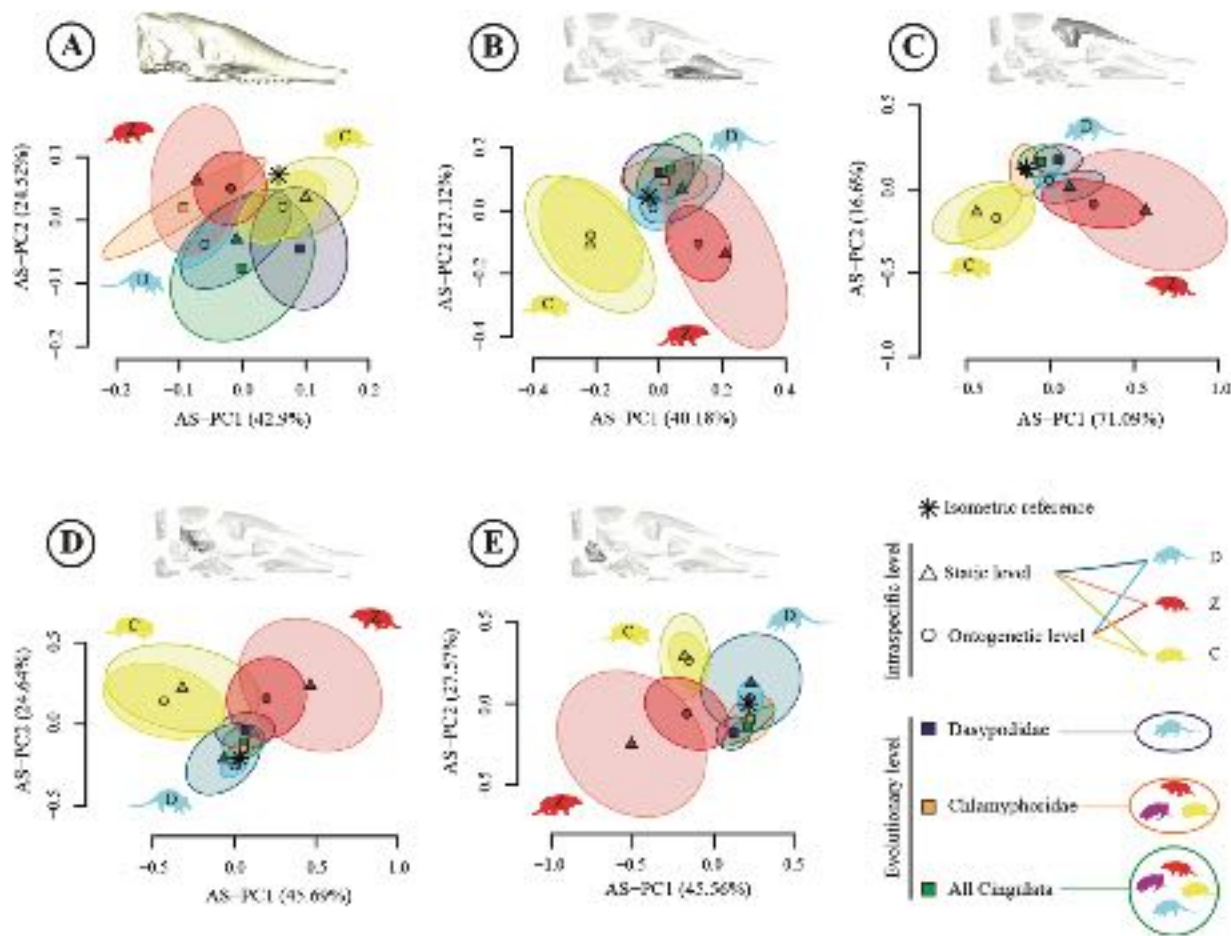


Figure 5. Principal component analysis of the allometric spaces (=AS) using slope coefficients and combining ontogenetic, static, and evolutionary levels of allometric variation for the entire cranium (A) and at the scale of the selected cranial subunits (see Figure 3): maxillary (B), frontal (C), squamosal (D), and petrosal (E) (see text). Allometric patterns are displayed with 95% confidence ellipses (250 bootstrap replicates). Abbreviations: C, *Cabassous*; D, *Dasypus*; Z, *Zaedyus*.

are altricial (Desbiez et al., 2018; McDonough et al., 1998; Meritt, 1985; Superina & Abba, 2014). Growth strategies are known to affect disparity in cranial shape more strongly for precocial mammals than for altricial ones (see Wilson, 2018; and references therein). Different developmental strategies might also explain differences in allometric strengths observed among developmental series, potentially explaining why *Dasypus*, with its longer growth period, has a higher ontogenetic allometry for the entire cranium than *Zaedyus* and *Cabassous*. However, this reasoning cannot apply to those cranial subunits (e.g., palatine, sphenopterygoid complex, jugal, premaxillary, and parietal) that show a greater allometric signal in *Zaedyus* and *Cabassous* than in *Dasypus*. Besides, these contrasted growth strategies may explain the greater difficulty of recognizing ontogenetic stages in *Zaedyus* and *Cabassous*.

Other developmental parameters, such as ossification patterns and tissue origin, might explain heterogeneous allometric strengths among cranial subunits in cingulates. Gonzalez et al. (2011) performed regionalized allometric analyses of the human cranium and showed that the face and vault had higher allometric strength than the basicranium. In our analysis, cranial subunits highly impacted by allometry are spread across the cranium, notably in the vault, but to the exclusion of the face. These subunits do not derive preferably from the

neural crest or mesoderm and ossify at different times during prenatal ontogeny (Hautier et al., 2011; Piekarski et al., 2014), which do not lend support to the existence of a link between tissue origin, ossification sequences and the distribution of allometric strength (*contra* Le Verger et al., 2020).

The pervasiveness and spatial expression of allometry

Size-related shape changes constitute a major component of morphological variation and integration (e.g., Gould, 1966; Hallgrímsson et al., 2019; Klingenberg, 2013, 2016; Mitteroecker & Bookstein, 2007; Porto et al., 2013). Here, we showed that size constitutes an important determinant of morphological variation in armadillos, by comparing allometric patterns (trajectories and shape changes) across variational levels. Allometric trajectories at the intraspecific level were significantly different among the three species at all anatomical scales. This contrasts with the comparison of evolutionary allometric trajectories, which hardly differed among families, except for a few cranial subunits. The fact that ontogenetic (and static) allometries differ but that evolutionary allometries do not is more difficult to interpret. Several studies have shown the existence of relatively low evolutionary allometry compared to lineage-specific patterns of diversification, as divergences or convergences among lineages could

be mainly explained by size-dependent ecological specializations (Friedman et al., 2019; Zelditch & Swiderski, 2022). In armadillos, diet or other ecological factors do not strictly distinguish the two families. The few allometric differences at the evolutionary level could thus be suggested by this weak ecological distinction among the lineages, but this interpretation remains speculative. Also, these contrasted patterns of trajectories might be explained by the differential sampling of the ontogenetic, static, and evolutionary levels, the latter being much less densely sampled than the two others ($N = 9\text{--}14$ (species) per family vs $N = 22\text{--}76$ (individuals) per species). However, it might simply be that allometries differ more among cingulate species than among cingulate families. In the present case, intraspecific allometries were compared among distantly related species, belonging to two different families (and three “subfamilies”). It may well be that allometries among distantly related species diverge more clearly than allometries of their respective families due to the greater evolutionary distance among the groups being compared in the former. Future research must determine whether these differing allometric trajectories across variational levels are the norm or an exception within mammals.

Although comparisons among and between levels revealed different allometric trajectories, our study highlights the existence of some allometric shape changes that are present in all investigated species, at all levels of variation, and at different anatomical scales (Supplementary Figures S4–S14). The iterative detection of some allometric shape changes at different variational levels meets a general observation, especially that of an alignment of static and evolutionary allometry (Hallgrímsson et al., 2019), although major exceptions also exist (Cheverud, 1982a; Cock, 1966; Lande, 1985; Voje et al., 2014). Our results clearly concur with this contrasted view by recovering both shared and unique patterns across species and levels.

An allometric shape change present at all levels of variation and/or at different anatomical scales implies a major trend of morphological variation in a given clade. The link between size and shape variation is not straightforward, and the interpretation of allometric shape changes present at multiple variational levels remains complex (Lande, 1979, 1985). A few studies have tentatively hypothesized the role of some driving selection processes in resolving the origin of integration patterns occurring at different levels, with allometry being only a special case of morphological integration (Hallgrímsson et al., 2019). Cheverud (1982a) and Gonzalez et al. (2011) proposed that common integration patterns between ontogenetic and static levels could be induced by a rapid growth strategy, although Pélabon et al. (2013) pointed out that a comparison of the two levels is probably more complex. On the other hand, Weaver et al. (2007) and Smith (2011) have suggested that common integration patterns between the static and evolutionary levels could simply derive from drift. Allometric patterns could then arise from a size-induced constraint on shape along a line of least resistance (Schluter, 1996; Voje et al., 2014). However, these hypotheses are challenged by numerous studies, showing that some of these patterns correspond to biological traits under selection (Adams & Nistri, 2010; Esquerré et al., 2017, 2022; Frankino et al., 2005; Giannini, 2014; Klingenberg, 2010; Porto et al., 2013; Wilson & Sánchez-Villagra, 2010). Such hypotheses remain largely underexplored and the characterization of the origin of allometry, and more broadly integration patterns, across

variational levels represents a promising avenue to decipher morphological variation during development and evolution (Klingenberg, 2014). Our study can hardly contribute to these debates, but our results suggest that some allometric shape changes are highly conserved or selected within cingulates.

Widespread allometric variations among the three variational levels explored imply that multiple levels of variation should be scrutinized. Klingenberg (2014) highlighted that the source of morphological variation may be a consequence of genetic, environmental, functional, or developmental factors. Alongside the categorization of variational levels, morphological variation should also be considered as a continuum, as evidenced by the intricacy of static, ontogenetic, and evolutionary levels and the pervasiveness of some allometric patterns. In the allometric space (Figure 5), the greater proximity between the slopes of the evolutionary level in cingulates and the intraspecific levels of *Dasybus*, as compared to those of *Cabassous* and *Zaedyus*, reinforces this assertion. Such intricacy might also apply to the different anatomical scales at which allometry is scrutinized. Our study solely focused on the entire cranium and cranial subunits, but similar allometric shape changes could also be present at other scales. For example, an allometric variation of the postorbital constriction was found both at the entire cranial and frontal bone scale and could probably be detected at the scale of the vault. Many studies have shown that morphological integration can be more concentrated in certain regions of an anatomical structure than between these same regions, leading to the definition of commonly accepted cranial modules in mammals (e.g., Bolker, 2000; Churchill et al., 2019; Goswami, 2006; Goswami & Finarelli, 2016; Goswami & Polly, 2010; Hallgrímsson et al., 2009; Klingenberg, 2005, 2008; Monteiro et al., 2005; Santana & Lofgren, 2013; Zelditch & Goswami, 2021), such as the vault. Modules could then represent a relevant intermediate anatomical scale to further disentangle cranial allometric patterns and explore their link to functional and developmental determinants of modularity and integration (Bissell & Diggle, 2010; Cheverud, 1982b; Olson & Miller, 1958; Wagner, 1996). The analysis of different scales has also shown unsuspected allometric shape changes shared among the variational levels, but not between the two anatomical scales. This reveals that analyses performed at a cranial scale may mask more local allometric shape changes and emphasize the need to scrutinize allometry at various anatomical scales.

The detection of unsuspected allometric shape changes at a more local scale is reminiscent of the palimpsest metaphor of Hallgrímsson et al. (2009) for integration and modularity, recently revisited through an evolutionary palimpsest according to Evans et al. (2022). Allometric shape changes occurring at different scales imply a superimposition of allometric patterns throughout the cranium, which could mask local allometric shape changes when looking at a global scale. Under this hypothesis, CREA-derived allometric shape changes expressed over the entire cranium would mask the more local non-CREA-derived allometric shape changes. An example supporting this hypothesis is the finding of the greater protrusion of the mastoid process at the petrosal scale and not at the cranial scale in which this variation is obscured by the relative reduction of the braincase. A limitation of this analogy is that the palimpsest, as defined by Hallgrímsson et al. (2009), describes how various subsequent developmental processes progressively leave covariation imprints that accumulate to

build a complex covariation structure. In the case of allometry, the processes involved are not clearly identified and may be complexified by the epigenetic response during growth in a composite structure like the skull (Hallgrímsson et al., 2007; Mitteroecker et al., 2020).

Conclusion and perspectives

The analysis of cranial allometry in armadillos demonstrates both the pervasiveness and complex expression of allometry across variational levels and anatomical scales. Our results show that the greater the phylogenetic distance between species, the greater the difference in their ontogenetic and static trajectories of allometric variation. The magnitude of these differences is also greater than that observed between the evolutionary allometric trajectories of the two families. Our analyses further revealed the spatial complexity of allometry on a composite structure such as the armadillo cranium. At the entire cranium level, the main shape change consisted of generalized craniofacial allometry accompanied by other newly detected allometric shape changes. More locally, repeated allometric shape changes were also detected for cranial subunits, unveiling size-correlated shape changes that went unnoticed at a more global scale. Beyond this spatial complexity, the discovery of widespread allometric variations within a clade like Cingulata clearly demonstrates the highly pervasive nature of allometry (Hallgrímsson et al., 2019) and further raises the question of its determinants.

Although our analyses provide a substantial report of cranial allometry in cingulates, our results encourage the exploration of allometric patterns at the evolutionary level with the inclusion of extinct taxa, such as representatives prone to gigantism like glyptodonts and pampatheres (Le Verger, 2023; Machado et al., 2022; Vizcaíno & Loughry, 2008). Such an investigation would be even more relevant to test the CREA hypothesis, given the unusual short face and dorsal position of the orbit found in Pleistocene glyptodonts (e.g., Machado et al., 2022). At a broader taxonomic scale, the widespread allometric variations detected here may be extended to xenarthrans as a whole and even to other mammalian clades.

Supplementary material

Supplementary material is available online at *Evolution*.

Data availability

All data related to the present study are given in the body of the text and as supplementary data, except for the 3D models and CT scans. For the latter, given the large amount of data, sharing will be done progressively after publication as follows: a large part of specimens scanned will be available on MorphoMuseum for 3D models and on MorphoSource for CT scans, both related to the present publication, including sharing specimens with Le Verger et al. (2020). Specimens CT scanned by L.R.G.R. will be available upon request to L.R.G.R.. The list of specimens is given in [Supplementary Table S1](#).

Author contributions

K.L.V. contributed to data acquisition, data analyses/interpretations, development of the approach, drafting of the manuscript, and study design. L.H. contributed to data

acquisition, development of the approach, and critical revision of the manuscript. S.G. and J.B. contributed to the analyses, development of the approach, and critical revision of the manuscript. F.D., L.R.G.R., and E.A. contributed to data acquisition and critical revision of the manuscript. G.B. contributed to data acquisition, development of the approach, study design, and critical revision of the manuscript.

Funding

Some of 3D data acquisitions were performed using the μ -CT facilities of the MRI platform member of the national infrastructure France-BioImaging supported by the French National Research Agency (ANR-10-INBS-04, “Investments for the future”), and of the Labex CEMEB (Centre Méditerranéen de l’Environnement et de la Biodiversité: ANR-10-LABX-0004) and NUMEV (Digital and hardware solutions for the environmental and life sciences: ANR-10-LABX-0020). This research received support from the Synthesys Project (<http://synthesys3.myspecies.info/>), which is funded by the European Community Research Infrastructure Action under the FP7. This is contribution ISEM 2020-202 of the ISEM. The fees for the OpenAccess publication of our work were covered by the 82918619 Consortium of Swiss Academic Libraries CSAL Open Access Agreement.

Conflict of interests: The authors declare no conflict of interests.

Acknowledgments

We are grateful to Christiane Denys, Violaine Nicolas, and Géraldine Véron (Muséum National d’Histoire Naturelle, MNHN, Paris, France); Roberto Portela Miguez, Louise Tomsett, and Laura Balcells (Natural History Museum, NHMUK, London, UK); Neil Duncan, Eileen Westwig, Eleanor Hoeger, Ross MacPhee, Marisa Surovy, and Morgan Hill Chase (American Museum of Natural History, AMNH, New York, USA); Nicole Edmison and Chris Helgen (National Museum of Natural History, NMNH, Washington, DC, USA); Jake Esselstyn (Louisiana State University, LSU, Museum of Natural Sciences, Baton Rouge, USA); Edward Stanley (University of Florida, UF, Florida Museum of Natural History, Gainesville, USA); Manuel Ruedi (Muséum d’Histoire Naturelle de Genève, MHNG, Geneva, Switzerland); Pepijn Kamminga, Arjen Speksnijder, Rob Langelaan, and Ate-Alma Cohen (Naturalis Biodiversity Center, NBC, Leiden, Holland); Steffen Bock, Christiane Funk, Frieder Mayer, Anna Rosemann, Lisa Jansen, Kristin Mahlow, and Johannes Müller (Museum für Naturkunde, ZMB, Berlin, Germany); Jacqueline Miller and Burton Lim (Royal Ontario Museum, ROM, Toronto, Canada); Olivier Pauwels and Jonathan Brecko (Royal Belgian Institute of Natural Sciences, RBINS, Brussels, Belgium); Stefan Merker (State Museum of Natural History, SMNH, Stuttgart, Germany); and Camille Grohé (University of Poitiers, UP, Poitiers, France) for access to comparative material and/or to CT scans. Many thanks to Sergio Ferreira-Cardoso (Institut des Sciences de l’Évolution de Montpellier, ISEM, Montpellier, France) for his help with data acquisition during the trips of K.L.V. and interesting discussions. Thanks also to Anderson Feijó (Chinese Academy of Sciences, CAS, Beijing, China) for discussions about the taxonomic validity of armadillo species and to Rémi Lefebvre (MNHN) for his help

with the definition of internal landmarks. We thank Benoit de Thoisy (Pasteur Institute of Guyana, Cayenne, French Guyana) and Clara Belfiore (not affiliated) for their help with data acquisition, and Olivia Plateau (University of Cambridge, UC, Cambridge, UK) for her help on the R script. We thank Renaud Lebrun (ISEM), Farah Ahmed (NHMUK), Miguel García-Sanz, Marta Bellato, Nathalie Poulet, and Florent Goussard (Platform AST-RX—MNHN) who generously provided help with CT scanning. We would like to warmly thank Christian de Muizon (MNHN), Timothy Gaudin (University of Tennessee at Chattanooga, UTC, Chattanooga, USA), Robert J. Asher (UC), Sophie Montuire (University of Bourgogne, UB, Dijon, France), Isabelle Rouget (MNHN), and Allowen Evin (ISEM) for reviewing a previous version of this work in the PhD dissertation of K.L.V. We would also like to thank Marcelo R. Sánchez-Villagra (University of Zurich, PIMUZ, Zurich, Switzerland) for his support during the finalization of the study.

References

- Abba, A. M., Cassini, G. H., Valverde, G., Tilak, M. K., Vizcaíno, S. F., Superina, M., & Delsuc, F. (2015). Systematics of hairy armadillos and the taxonomic status of the Andean hairy armadillo (*Chaetophractus nationi*). *Journal of Mammalogy*, 96(4), 673–689. <https://doi.org/10.1093/jmammal/gyv082>
- Adams, D. C., & Collyer, M. L. (2018). Phylogenetic ANOVA: Group-clade aggregation, biological challenges, and a refined permutation procedure. *Evolution*, 72(6), 1204–1215. <https://doi.org/10.1111/evo.13492>
- Adams, D. C., Collyer, M. L., Kaliontzopoulou, A., & Baken, E. (2022). *Geomorph: Software for geometric morphometric analyses*. R package version 4.0.4. <https://cran.r-project.org/package=geomorph>
- Adams, D. C., & Nistri, A. (2010). Ontogenetic convergence and evolution of foot morphology in European cave salamanders (Family: Plethodontidae). *BMC Evolutionary Biology*, 10, 216–226. <https://doi.org/10.1186/1471-2148-10-216>
- Adams, D. C., Rohlf, F. J., & Slice, D. E. (2013). A field comes of age: geometric morphometrics in the 21st century. *Hystrix, the Italian Journal of Mammalogy*, 24(1), 7–14. <https://doi.org/10.4404/hystrix-24.1-6283>
- Arteaga, M. C., Gasca-Pineda, J., Bello-Bedoy, R., Eguiarte, L. E., & Medellín, R. A. (2020). Conservation genetics, demographic history, and climatic distribution of the nine-banded armadillo (*Dasyops novemcinctus*): An analysis of its mitochondrial lineages. In J. Ortega, & J. E. Maldonado (Eds.), *Conservation genetics in mammals: Integrative research using novel approaches* (pp. 141–163). Springer. https://doi.org/10.1007/978-3-030-33334-8_7
- Baken, E., Collyer, M. L., Kaliontzopoulou, A., & Adams, D. C. (2021). geomorph v40 and gmShiny: Enhanced analytics and a new graphical interface for a comprehensive morphometric experience. *Methods in Ecology and Evolution*, 12(12), 2355–2363. <https://doi.org/10.1111/2041-210X.13723>
- Billet, G., & Bardin, J. (2019). Serial homology and correlated characters in morphological phylogenetics: Modeling the evolution of dental crests in placentals. *Systematic Biology*, 68(2), 267–280. <https://doi.org/10.1093/sysbio/syy071>
- Billet, G., & Bardin, J. (2021). Segmental series and size: Clade-wide investigation of molar proportions reveals a major evolutionary allometry in the dentition of placental mammals. *Systematic Biology*, 70(6), 1101–1109. <https://doi.org/10.1093/sysbio/syab007>
- Billet, G., Hautier, L., Thoisy, de B., & Delsuc, F. (2017). The hidden anatomy of paranasal sinuses reveals biogeographically distinct morphotypes in the nine-banded armadillo (*Dasyops novemcinctus*). *PeerJ*, 5, e3593. <https://doi.org/10.7717/peerj.3593>
- Billet, G., Muizon, de C., Schellhorn, R., Ruf, I., Ladevèze, S., & Bergqvist, L. (2015). Petrosal and inner ear anatomy and allometry amongst specimens referred to Litopterna (Placentalia). *Zoological Journal of the Linnean Society*, 173(4), 956–987. <https://doi.org/10.1111/zoj.12219>
- Bissell, E. K., & Diggle, P. K. (2010). Modular genetic architecture of floral morphology in *Nicotiana*: quantitative genetic and comparative phenotypic approaches to floral integration. *Journal of Evolutionary Biology*, 23(8), 1744–1758. <https://doi.org/10.1111/j.1420-9101.2010.02040.x>
- Bolker, J. A. (2000). Modularity in development and why it matters to evo-devo. *American Zoologist*, 40(5), 770–776. <https://doi.org/10.1093/icb/40.5.770>
- Cardini, A. (2019a). Craniofacial allometry is a rule in evolutionary radiations of placentals. *Evolutionary Biology*, 46(3), 239–248. <https://doi.org/10.1007/s11692-019-09477-7>
- Cardini, A. (2019b). Integration and modularity in Procrustes shape data: Is there a risk of spurious results? *Evolutionary Biology*, 46(1), 90–105. <https://doi.org/10.1007/s11692-018-9463-x>
- Cardini, A., & Polly, P. D. (2013). Larger mammals have longer faces because of size-related constraints on skull form. *Nature Communications*, 4(1), 2458. <https://doi.org/10.1038/ncomms3458>
- Cardini, A., Polly, P. D., Dawson, R., & Milne, N. (2015). Why the long face? Kangaroos and wallabies follow the same ‘rule’ of cranial evolutionary allometry (CREA) as placentals. *Evolutionary Biology*, 42, 169–176. <https://doi.org/10.1007/s11692-015-9308-9>
- Carlini, A. A., Soibelzon, E., & Glaz, D. (2016). *Chaetophractus velerosus* (Cingulata: Dasypodidae). *Mammalian Species*, 48(937), 73–82. <https://doi.org/10.1093/mspecies/sew008>
- Chatterji, R. M., Hipsley, C. A., Sherratt, E., Hutchinson, M. N., & Jones, M. E. (2022). Ontogenetic allometry underlies trophic diversity in sea turtles (Chelonioidae). *Evolutionary Ecology*, 36(4), 511–540. <https://doi.org/10.1007/s10682-022-10162-z>
- Cheverud, J. M. (1982a). Relationships among ontogenetic, static, and evolutionary allometry. *American Journal of Physical Anthropology*, 59(2), 139–149. <https://doi.org/10.1002/ajpa.1330590204>
- Cheverud, J. M. (1982b). Phenotypic, genetic, and environmental morphological integration in the cranium. *Evolution*, 36(3), 499–516. <https://doi.org/10.1111/j.1558-5646.1982.tb05070.x>
- Churchill, M., Miguel, J., Beatty, B. L., Goswami, A., & Geisler, J. H. (2019). Asymmetry drives modularity of the skull in the common dolphin (*Delphinus delphis*). *Biological Journal of the Linnean Society*, 126(2), 225–239. <https://doi.org/10.1093/biolinnean/bly190>
- Ciancio, M. R., Castro, M. C., Galliari, F. C., Carlini, A. A., & Asher, R. J. (2012). Evolutionary implications of dental eruption in *Dasyops* (Xenarthra). *Journal of Mammalian Evolution*, 19(1), 1–8. <https://doi.org/10.1007/s10914-011-9177-7>
- Cock, A. G. (1966). Genetical aspects of metrical growth and form in animals. *The Quarterly Review of Biology*, 41(2), 131–190. <https://doi.org/10.1086/404940>
- Collyer, M. L., & Adams, D. C. (2018). RRPP: An R package for fitting linear models to high-dimensional data using residual randomization. *Methods in Ecology and Evolution*, 9(7), 1772–1779. <https://doi.org/10.1111/2041-210X.13029>
- Collyer, M. L., & Adams, D. C. (2021). RRPP: Linear Model Evaluation with Randomized Residuals in a Permutation Procedure. R package version 1.1.2. <https://cran.r-project.org/package=RRPP>
- Delsuc, F., Gibb, G. C., Kuch, M., Billet, G., Hautier, L., Southon, J., Rouillard, J. M., Fernicola, J. C., Vizcaíno, S. F., MacPhee, R. D. E., & Poinar, H. N. (2016). The phylogenetic affinities of the extinct glyptodonts. *Current Biology*, 26(4), 155–156. <https://doi.org/10.1016/j.cub.2016.01.039>
- Desbiez, A. L. J., Massocato, G. F., Kluyber, D., & Fernandes Santos, R. C. (2018). Unraveling the cryptic life of the southern naked-tailed armadillo, *Cabassous unicinctus squamicaudis* (Lund, 1845), in a Neotropical wetland: home range, activity pattern, burrow use and reproductive behaviour. *Mammalian Biology*, 91, 95–103. <https://doi.org/10.1016/j.mambio.2018.02.006>
- Desmarest, A. G. (1804). *Nouveau dictionnaire d'histoire naturelle, appliquée aux arts, principalement à l'agriculture et à l'économie*

- rurale et domestique: par une société de naturalistes et d'agriculteurs: avec des figures tirées des trois règnes de la nature.* Chez Deterville.
- Drake, A. G., & Klingenberg, C. P. (2008). The pace of morphological change: Historical transformation of skull shape in St Bernard dogs. *Proceedings of the Royal Society B: Biological Sciences*, 275(1630), 71–76. <https://doi.org/10.1098/rspb.2007.1169>
- Esquerré, D., Keogh, J. S., Demangel, D., Morando, M., Avila, L. J., Sites Jr, J. W., Ferri-Yañez, F., & Leaché, A. D. (2022). Rapid radiation and rampant reticulation: Phylogenomics of South American *Liolaemus* lizards. *Systematic Biology*, 71(2), 286–300. <https://doi.org/10.1093/sysbio/syab058>
- Esquerré, D., Sherratt, E., & Keogh, J. S. (2017). Evolution of extreme ontogenetic allometric diversity and heterochrony in pythons, a clade of giant and dwarf snakes. *Evolution*, 71(12), 2829–2844. <https://doi.org/10.1111/evo.13382>
- Evans, K. M., Buser, T. J., Larouche, O., & Kolmann, M. A. (2022). Untangling the relationship between developmental and evolutionary integration. *Seminars in Cell & Developmental Biology*, 145, 22–27. <https://doi.org/10.1016/j.semedb.2022.05.026>
- Feijó, A., & Anacleto, T. C. (2021). Taxonomic revision of the genus *Cabassous* McMurtrie, 1831 (Cingulata: Chlamyphoridae), with revalidation of *Cabassous squamicaudis* (Lund, 1845). *Zootaxa*, 4974(1), 47–78. <https://doi.org/10.11646/zootaxa.4974.1.2>
- Feijó, A., Patterson, B. D., & Cordeiro-Estrela, P. (2018). Taxonomic revision of the long-nosed armadillos, Genus *Dasybus* Linnaeus, 1758 (Mammalia, Cingulata). *PLoS One*, 13(4), e0195084. <https://doi.org/10.1371/journal.pone.0195084>
- Feijó, A., Vilela, J. F., Cheng, J., Schetino, M. A. A., Coimbra, R. T. F., Bonvicino, C. R., Santos, F. R., Patterson, B. D., & Cordeiro-Estrela, P. (2019). Phylogeny and molecular species delimitation of long-nosed armadillos (*Dasybus*: Cingulata) supports morphology-based taxonomy. *Zoological Journal of the Linnean Society*, 186(3), 813–825. <https://doi.org/10.1093/zoolinnean/zly091>
- Felsenstein, J. (1985). Phylogenies and the comparative method. *The American Naturalist*, 125(1), 1–15. <https://doi.org/10.1086/284325>
- Ferreira-Cardoso, S., Billet, G., Gaubert, P., Delsuc, F., & Hautier, L. (2019). Skull shape variation in extant pangolins (Pholidota: Manidae): Allometric patterns and systematic implications. *Zoological Journal of the Linnean Society*, 188(1), 255–275. <https://doi.org/10.1093/zoolinnean/zlz096>
- Frankino, W. A., Zwaan, B. J., Stern, D. L., & Brakefield, P. M. (2005). Natural selection and developmental constraints in the evolution of allometries. *Science*, 307(5710), 718–720. <https://doi.org/10.1126/science.1105409>
- Friedman, S. T., Martinez, C. M., Price, S. A., & Wainwright, P. C. (2019). The influence of size on body shape diversification across Indo-Pacific shore fishes. *Evolution*, 73(9), 1873–1884. <https://doi.org/10.1111/evo.13755>
- Frost, S. R., Marcus, L. F., Bookstein, F. L., Reddy, D. P., & Delson, E. (2003). Cranial allometry, phylogeography, and systematics of large-bodied papionins (primates: Cercopithecinae) inferred from geometric morphometric analysis of landmark data. *The Anatomical Record Part A: Discoveries in Molecular, Cellular, and Evolutionary Biology*, 275A(2), 1048–1072. <https://doi.org/10.1002/ara.10112>
- Gerber, S., Eble, G. J., & Neige, P. (2008). Allometric space and allometric disparity: A developmental perspective in the macroevolutionary analysis of morphological disparity. *Evolution*, 62(6), 1450–1457. <https://doi.org/10.1111/j.1558-5646.2008.00370.x>
- Gerber, S., & Hopkins, M. J. (2011). Mosaic heterochrony and evolutionary modularity: The trilobite genus *Zacanthopsis* as a case study. *Evolution*, 65(11), 3241–3252. <https://doi.org/10.1111/j.1558-5646.2011.01363.x>
- Giannini, N. P. (2014). Quantitative developmental data in a phylogenetic framework. *Journal of Experimental Zoology. Part B. Molecular and Developmental Evolution*, 322(8), 558–566. <https://doi.org/10.1002/jez.b.22588>
- Giannini, N. P., Morales, M. M., Wilson, L. A., Velazco, P. M., Abdala, F., & Flores, D. A. (2021). The cranial morphospace of extant marsupials. *Journal of Mammalian Evolution*, 28(4), 1145–1160. <https://doi.org/10.1007/s10914-021-09589-y>
- Gibb, G. C., Condamine, F. L., Kuch, M., Enk, J., Moraes-Barros, N., Superina, M., Poinar, H. N., & Delsuc, F. (2016). Shotgun mitogenomics provides a reference phylogenetic framework and timescale for living xenarthrans. *Molecular Biology and Evolution*, 33(3), 621–642. <https://doi.org/10.1093/molbev/msv250>
- Gonzalez, P. N., Perez, S. I., & Bernal, V. (2011). Ontogenetic allometry and cranial shape diversification among human populations from South America. *Anatomical Record*, 294(11), 1864–1874. <https://doi.org/10.1002/ar.21454>
- Goodall, C. (1991). Procrustes methods in the statistical analysis of shape. *Journal of the Royal Statistical Society: Series B (Methodological)*, 53(2), 285–321. <https://doi.org/10.1111/j.2517-6161.1991.tb01825.x>
- Goswami, A. (2006). Cranial modularity shifts during mammalian evolution. *The American Naturalist*, 168(2), 270–280. <https://doi.org/10.1086/505758>
- Goswami, A., & Finarelli, J. A. (2016). EMLLi: A maximum likelihood approach to the analysis of modularity. *Evolution*, 70(7), 1622–1637. <https://doi.org/10.1111/evo.12956>
- Goswami, A., & Polly, P. D. (2010). The influence of modularity on cranial morphological disparity in Carnivora and Primates (Mammalia). *PLoS One*, 5(3), e9517. <https://doi.org/10.1371/journal.pone.0009517>
- Goswami, A., Smaers, J. B., Soligo, C., & Polly, P. D. (2014). The macroevolutionary consequences of phenotypic integration: From development to deep time. *Philosophical Transactions of the Royal Society B: Biological Sciences*, 369(1649), 20130254. <https://doi.org/10.1098/rstb.2013.0254>
- Gould, S. J. (1966). Allometry and size in ontogeny and phylogeny. *Biological Reviews of the Cambridge Philosophical Society*, 41(4), 587–640. <https://doi.org/10.1111/j.1469-185x.1966.tb01624.x>
- Gould, S. J. (1975). Allometry in primates, with emphasis on scaling and evolution of brain. *Contributions to Primatology*, 5, 244–292.
- Gould, S. J. (1989). A developmental constraint in *Cerion*, with comments on the definition and interpretation of constraint in evolution. *Evolution*, 43(3), 516–539. <https://doi.org/10.1111/j.1558-5646.1989.tb04249.x>
- Gray, J. E. (1865). Revision of the genera and species of entomophagous Edentata, founded on the examination of the specimens in the British Museum. *Proceedings of the Zoological Society of London*, 33(1), 359–386. <https://doi.org/10.1111/j.1469-7998.1865.tb02351.x>
- Hallgrímsson, B., Jamniczky, H., Young, N. M., Rolian, C., Parsons, T. E., Boughner, J. C., & Marcucio, R. S. (2009). Deciphering the palimpsest: Studying the relationship between morphological integration and phenotypic covariation. *Evolutionary Biology*, 36(4), 355–376. <https://doi.org/10.1007/s11692-009-9076-5>
- Hallgrímsson, B., Katz, D. C., Aponte, J. D., Larson, J. R., Devine, J., Gonzalez, P. N., Young, N. M., Roseman, C. C., & Marcucio, R. S. (2019). Integration and the developmental genetics of allometry. *Integrative and Comparative Biology*, 59(5), 1369–1381. <https://doi.org/10.1093/icb/icz105>
- Hallgrímsson, B., Lieberman, D. E., Liu, W., Ford-Hutchinson, A. F., & Jirik, F. R. (2007). Epigenetic interactions and the structure of phenotypic variation in the cranium. *Evolution & Development*, 9(1), 76–91. <https://doi.org/10.1111/j.1525-142x.2006.00139.x>
- Hallgrímsson, B., Percival, C. J., Green, R., Young, N. M., Mio, W., & Marcucio, R. (2015). Morphometrics, 3D imaging, and craniofacial development. *Current Topics in Developmental Biology*, 115, 561–597. <https://doi.org/10.1016/bs.ctdb.2015.09.003>
- Hautier, L., Billet, G., De Thoisy, B., & Delsuc, F. (2017). Beyond the carapace: Skull shape variation and morphological systematics of long-nosed armadillos (genus *Dasybus*). *PeerJ*, 5, e3650. <https://doi.org/10.7717/peerj.3650>
- Hautier, L., Weisbecker, V., Goswami, A., Knight, F., Kardjilov, N., & Asher, R. J. (2011). Skeletal ossification and sequence heterochrony

- in Xenarthran evolution. *Evolution and Development*, 13(5), 460–476. <https://doi.org/10.1111/j.1525-142X.2011.00503.x>
- Haysen, V. (2014). *Cabassous unicinctus* (Cingulata: Dasypodidae). *Mammalian Species*, 46(907), 16–23. <https://doi.org/10.1644/907>
- Hubbe, A., Melo, D., & Marroig, G. (2016). A case study of extant and extinct Xenarthra cranium covariance structure: Implications and applications to paleontology. *Paleobiology*, 42(3), 465–488. <https://doi.org/10.1017/pab.2015.49>
- Huchon, D., Delsuc, F., Catzeflis, F. M., & Douzery, E. J. (1999). Armadillos exhibit less genetic polymorphism in North America than in South America: Nuclear and mitochondrial data confirm a founder effect in *Dasybus novemcinctus* (Xenarthra). *Molecular Ecology*, 8(10), 1743–1748. <https://doi.org/10.1046/j.1365-294x.1999.00768.x>
- Isler, K., & van Schaik, C. P. (2009). The expensive brain: A framework for explaining evolutionary changes in brain size. *Journal of Human Evolution*, 57(4), 392–400. <https://doi.org/10.1016/j.jhevol.2009.04.009>
- Klingenberg, C. P. (1996). Multivariate allometry. In L. F. Marcus, M. Corti, A. Loy, G. J. P. Naylor, & D. E. Slice (Eds.), *Advances in morphometrics* (pp. 23–49). Springer. https://doi.org/10.1007/978-1-4757-9083-2_3
- Klingenberg, C. P. (2005). Developmental constraints, modules, and evolvability. In B. Hallgrímsson, & B. Hall (Eds.), *Variation* (pp. 219–247). Academic Press. <https://doi.org/10.1016/B978-012088777-4/50013-2>
- Klingenberg, C. P. (2008). Morphological integration and developmental modularity. *Annual Review of Ecology, Evolution, and Systematics*, 39(1), 115–132. <https://doi.org/10.1146/annurev.ecolsys.37.091305.110054>
- Klingenberg, C. P. (2010). Evolution and development of shape: Integrating quantitative approaches. *Nature Reviews Genetics*, 11(9), 623–635. <https://doi.org/10.1038/nrg2829>
- Klingenberg, C. P. (2013). Cranial integration and modularity: Insights into evolution and development from morphometric data. *Hystrix*, 24(1), 43–58. <https://doi.org/10.4404/hystrix-24.1-6367>
- Klingenberg, C. P. (2014). Studying morphological integration and modularity at multiple levels: Concepts and analysis. *Philosophical Transactions of the Royal Society B: Biological Sciences*, 369(1649), 20130249. <https://doi.org/10.1098/rstb.2013.0249>
- Klingenberg, C. P. (2016). Size, shape, and form: Concepts of allometry in geometric morphometrics. *Development Genes and Evolution*, 226(3), 113–137. <https://doi.org/10.1007/s00427-016-0539-2>
- Klingenberg, C. P., Barluenga, M., & Meyer, A. (2002). Shape analysis of symmetric structures: Quantifying variation among individuals and asymmetry. *Evolution*, 56(10), 1909–1920. <https://doi.org/10.1111/j.0014-3820.2002.tb00117.x>
- Klingenberg, C. P., Duttke, S., Whelan, S., & Kim, M. (2012). Developmental plasticity, morphological variation and evolvability: A multilevel analysis of morphometric integration in the shape of compound leaves. *Journal of Evolutionary Biology*, 25(1), 115–129. <https://doi.org/10.1111/j.1420-9101.2011.02410.x>
- Klingenberg, C. P., & Marugán-Lobón, J. (2013). Evolutionary covariation in geometric morphometric data: Analyzing integration, modularity, and allometry in a phylogenetic context. *Systematic Biology*, 62(4), 591–610. <https://doi.org/10.1093/sysbio/syt025>
- Klingenberg, C. P., & Zimmermann, M. (1992). Static, ontogenetic, and evolutionary allometry: A multivariate comparison in nine species of water striders. *The American Naturalist*, 140(4), 601–620. <https://doi.org/10.1086/285430>
- Kyomen, S., Murillo-Rincón, A. P., & Kaucká, M. (2023). Evolutionary mechanisms modulating the mammalian skull development. *Philosophical Transactions of the Royal Society B: Biological Sciences*, 378(1880), 20220080. <http://doi.org/10.1098/rstb.2022.0080>
- Lande, R. (1979). Quantitative genetic analysis of multivariate evolution, applied to brain: Body size allometry. *Evolution*, 33(1Part2), 402–416. <https://doi.org/10.1111/j.1558-5646.1979.tb04694.x>
- Lande, R. (1985). Genetic and evolutionary aspects of allometry. In W. L. Jungers (Ed.), *Size and scaling in primate biology. Advances in primatology*. Springer (pp. 21–32). https://doi.org/10.1007/978-1-4899-3647-9_2
- Le Verger, K. (2023). Xenarthrans of the collection of Santiago Roth from the Pampean Region of Argentina (Pleistocene), in Zurich, Switzerland. *Swiss Journal of Palaeontology*, 142(1), 1–39. <https://doi.org/10.1186/s13358-023-00265-7>
- Le Verger, K., Hautier, L., Bardin, J., Gerber, S., Delsuc, F., & Billet, G. (2020). Ontogenetic and static allometry in the skull and cranial units of nine-banded armadillos (Cingulata: Dasypodidae: *Dasybus novemcinctus*). *Biological Journal of the Linnean Society*, 131(3), 673–698. <https://doi.org/10.1093/biolinnean/blaa083>
- Linnæus, C. (1758). *Systema naturae per regna tria naturæ, secundum classes, ordines, genera, species, cum characteribus, differentiis, synonymis, locis. Tomus I. Editio decima, reformata*. Homiae: Laurentii Salvii.
- Lönnerberg, E. (1942). *Notes on Xenarthra from Brazil and Bolivia*. Almqvist & Wiksell.
- Machado, F. A., Marroig, G., & Hubbe, A. (2022). The pre-eminent role of directional selection in generating extreme morphological change in glyptodonts (Cingulata; Xenarthra). *Proceedings of the Royal Society B: Biological Sciences*, 289(1967), 20212521. <https://doi.org/10.1098/rspb.2021.2521>
- Marcy, A. E., Guillerme, T., Sherratt, E., Rowe, K. C., Phillips, M. J., & Weisbecker, V. (2020). Australian rodents reveal conserved cranial evolutionary allometry across 10 million years of murid evolution. *The American Naturalist*, 196(6), 755–768. <https://doi.org/10.1086/711398>
- McDonough, C. M. (2000). Social organization of nine-banded armadillos (*Dasybus novemcinctus*) in a riparian habitat. *The American Midland Naturalist*, 144(1), 139–151. [https://doi.org/10.1674/0003-0031\(2000\)144\[0139:soonba\]2.0.co;2](https://doi.org/10.1674/0003-0031(2000)144[0139:soonba]2.0.co;2)
- McDonough, C. M., & Loughry, W. J. (2018). Family dasypodidae (long-nosed armadillos). In R. A. Mittermeier, & D. E. Wilson (Eds.), *Handbook of the mammals of the world: Insectivores, sloths and colungos* (pp. 30–47). Lynx edicions.
- McDonough, C. M., McPhee, S. A., & Loughry, W. J. (1998). Growth rates of juvenile nine-banded armadillos. *The Southwestern Naturalist*, 43(4), 462–468. <http://www.jstor.org/stable/30054084>
- Meritt, D. A., Jr. (1985). Naked-tailed armadillos, *Cabassous* sp. In G. G. Montgomery (Ed.), *The evolution and ecology of armadillos, sloths, and vermilinguas* (pp. 389–392). Smithsonian Institution Press.
- Miller, G. S. (1899). Notes on the naked-tailed armadillos. *Proceedings of the Biological Society of Washington*, 13, 1–8.
- Mitteroecker, P., Bartsch, S., Erkiner, C., Grunstra, N. D. S., Le Maître, A., & Bookstein, F. L. (2020). Morphometric variation at different spatial scales: Coordination and compensation in the emergence of organismal form. *Systematic Biology*, 69(5), 913–926. <https://doi.org/10.1093/sysbio/syaa007>
- Mitteroecker, P., & Bookstein, F. (2007). The conceptual and statistical relationship between modularity and morphological integration. *Systematic Biology*, 56(5), 818–836. <https://doi.org/10.1080/10635150701648029>
- Moeller, W. (1968). Allometrische analyse der gürteltier schädel Ein beitrage zur phylogenie der Dasypodidae Bonaparte, 1838. *Zoologische Jahrbücher. Abteilung für Anatomie und Ontogenie der Tiere*, 85, 411–528.
- Mondolfi, E. (1968). Descripción de un nuevo armadillo del género *Dasybus* de Venezuela (Mammalia-Edentata). *Memoria de la Sociedad Ciencias Naturales La Salle*, 27, 149–167.
- Monteiro, L. R. (1999). Multivariate regression models and geometric morphometrics: The search for causal factors in the analysis of shape. *Systematic Biology*, 48(1), 192–199. <https://doi.org/10.1080/106351599260526>. <https://www.jstor.org/stable/2585275>
- Monteiro, L. R., Bonato, V., & Dos Reis, S. F. (2005). Evolutionary integration and morphological diversification in complex morphological structures: mandible shape divergence in spiny rats (Rodentia, Echimyidae). *Evolution & Development*, 7(5), 429–439. <https://doi.org/10.1111/j.1525-142X.2005.05047.x>

- Olson, E. C., & Miller, R. L. (1958). *Morphological integration*. University of Chicago Press.
- Osborn, H. F. (1912). Skull measurements in man and the hoofed mammals. *Science*, 35(902), 1–596.
- Pélabon, C., Bolstad, G. H., Egset, C. K., Cheverud, J. M., Pavlicev, M., & Rosenqvist, G. (2013). On the relationship between ontogenetic and static allometry. *The American Naturalist*, 181(2), 195–212. <https://doi.org/10.1086/668820>
- Pélabon, C., Firmat, C. J. P., Bolstad, G. H., Voje, K. L., Houle, D., Cassara, J., Le Rouzic, A., & Hansen, T. F. (2014). Evolution of morphological allometry. *Annals of the New York Academy of Sciences*, 1320(1), 58–75. <https://doi.org/10.1111/nyas.12470>
- Phillips, M. J., Celik, M. A., & Beck, R. M. (2023). The evolutionary relationships of Diprotodontia and improving the accuracy of phylogenetic inference from morphological data. *Alcheringa: An Australasian Journal of Palaeontology*, 47(4), 686–698. <https://doi.org/10.1080/03115518.2023.2184492>
- Piekarski, N., Gross, J. B., & Hanken, J. (2014). Evolutionary innovation and conservation in the embryonic derivation of the vertebrate skull. *Nature Communications*, 5(1), 5661. <https://doi.org/10.1038/ncomms6661>
- Piras, P., Salvi, D., Ferrara, G., Maiorino, L., Delfino, M., Pedde, L., & Kotsakis, T. (2011). The role of post-natal ontogeny in the evolution of phenotypic diversity in *Podarcis* lizards. *Journal of Evolutionary Biology*, 24(12), 2705–2720. <https://doi.org/10.1111/j.1420-9101.2011.02396.x>
- Porto, A., Shirai, L. T., De Oliveira, F. B., & Marroig, G. (2013). Size variation, growth strategies, and the evolution of modularity in the mammalian skull. *Evolution*, 67(11), 3305–3322. <https://doi.org/10.1111/evo.12177>
- R Core Team. (2021). *R: A language and environment for statistical computing*. R Foundation for Statistical Computing. <https://www.R-project.org/>
- Radinsky, L. (1984a). Ontogeny and phylogeny in horse skull evolution. *Evolution*, 38(1), 1–15. <https://doi.org/10.1111/j.1558-5646.1984.tb00254.x>
- Radinsky, L. B. (1982). Evolution of skull shape in carnivores. 3. The origin and early radiation of the modern carnivore families. *Paleobiology*, 8(3), 177–195. <https://doi.org/10.1017/s0094837300006928>
- Radinsky, L. B. (1984b). Basicranial axis length v skull length in analysis of carnivore skull shape. *Biological Journal of the Linnean Society*, 22(1), 31–41. <https://doi.org/10.1111/j.1095-8312.1984.tb00797.x>
- Radinsky, L. B. (1985). Approaches in evolutionary morphology: A search for patterns. *Annual Review of Ecology and Systematics*, 16(1), 1–14. <https://doi.org/10.1146/annurev.es.16.110185.000245>. <https://www.jstor.org/stable/2097040>
- Robb, R. C. (1935a). A study of mutations in evolution I. Evolution in the equine skull. *Journal of Genetics*, 31(1), 39–46.
- Robb, R. C. (1935b). A study of mutations in evolution II. Ontogeny in the equine skull. *Journal of Genetics*, 31(1), 47–52.
- Rohlf, F. J. (2001). Comparative methods for the analysis of continuous variables: Geometric interpretations. *Evolution*, 55(11), 2143–2160. <https://doi.org/10.1111/j.0014-3820.2001.tb00731.x>
- Rohlf, F. J., & Slice, D. (1990). Extensions of the Procrustes method for the optimal superimposition of landmarks. *Systematic Zoology*, 39(1), 40–59. <https://doi.org/10.2307/2992207>
- Santana, S. E., & Lofgren, S. E. (2013). Does nasal echolocation influence the modularity of the mammal skull? *Journal of Evolutionary Biology*, 26(11), 2520–2526. <https://doi.org/10.1111/jeb.12235>
- Schlager, S. (2017). Morpho and rvcg—Shape analysis in R: R-packages for geometric morphometrics, shape analysis and surface manipulations. In G. Zheng, S. Li, & G. Székely (Eds.), *Statistical shape and deformation analysis* (pp. 217–256). Academic Press. <https://doi.org/10.1016/B978-0-12-810493-4.00011-0>
- Schluter, D. (1996). Adaptive radiation along genetic lines of least resistance. *Evolution*, 50(5), 1766–1774. <https://doi.org/10.1111/j.1558-5646.1996.tb03563.x>
- Schneider, C. A., Rasband, W. S., & Eliceiri, K. W. (2012). NIH Image to ImageJ: 25 years of image analysis. *Nature Methods*, 9(7), 671–675. <https://doi.org/10.1038/nmeth.2089>
- Sidlauskas, B. (2008). Continuous and arrested morphological diversification in sister clades of characiform fishes: A phylomorphospace approach. *Evolution*, 62(12), 3135–3156. <https://doi.org/10.1111/j.1558-5646.2008.00519.x>
- Silveira, L., de Almeida Jácomo, A. T., Furtado, M. M., Torres, N. M., Sollmann, R., & Vynne, C. (2009). Ecology of the giant armadillo (*Priodontes maximus*) in the grasslands of central Brazil. *Edentata*, 8-10(10), 25–34. <https://doi.org/10.1896/020.010.0112>
- Simons, E. A., & Frost, S. R. (2020). Ontogenetic allometry and scaling in catarrhine crania. *Journal of Anatomy*, 238(3), 693–710. <https://doi.org/10.1111/joa.13331>
- Smith, H. F. (2011). The role of genetic drift in shaping modern human cranial evolution: A test using microevolutionary modeling. *International Journal of Evolutionary Biology*, 145262, 1–7. <https://doi.org/10.4061/2011/145262>
- Squarcia, S. M., Sidorkewicz, N. S., Camina, R., & Casanave, E. B. (2009). Sexual dimorphism in the mandible of the armadillo *Chaetophractus villosus* (Desmarest, 1804) (Dasypodidae) from northern Patagonia, Argentina. *Brazilian Journal of Biology*, 69(2), 347–352. <https://doi.org/10.1590/s1519-69842009000200016>
- Strelin, M. M., Benitez-Vieyra, S. M., Fornoni, J., Klingenberg, C. P., & Cocucci, A. A. (2016). Exploring the ontogenetic scaling hypothesis during the diversification of pollination syndromes in *Caiophora* (Loasaceae, subfam Loasoideae). *Annals of Botany*, 117(5), 937–947. <https://doi.org/10.1093/aob/mcw035>
- Superina, M., & Abba, A. M. (2014). *Zaedyus pichiy* (Cingulata: Dasypodidae). *Mammalian Species*, 46(905), 1–10. <https://doi.org/10.1644/905.1>
- Superina, M., & Abba, A. M. (2018). Family Chlamyphoridae (Chlamyphorid armadillos). In R. A. Mittermeier, & D. E. Wilson (Eds.), *Handbook of the mammals of the world: Insectivores, sloths and colungos* (pp. 48–73). Lynx edicions.
- Tamagnini, D., Meloro, C., & Cardini, A. (2017). Anyone with a long-face? Craniofacial evolutionary allometry (CREA) in a family of short-faced mammals, the Felidae. *Evolutionary Biology*, 44(4), 476–495. <https://doi.org/10.1007/s11692-017-9421-z>
- Urošević, A., Ljubisavljević, K., & Ivanović, A. (2013). Patterns of cranial ontogeny in lacertid lizards: Morphological and allometric disparity. *Journal of Evolutionary Biology*, 26(2), 399–415. <https://doi.org/10.1111/jeb.12059>
- Urošević, A., Ljubisavljević, K., & Ivanović, A. (2018). Multilevel assessment of the lacertid lizard cranial modularity. *Journal of Zoological Systematics and Evolutionary Research*, 57(1), 145–158. <https://doi.org/10.1111/jzs.12245>
- Uyeda, J. C., Zenil-Ferguson, R., & Pennell, M. W. (2018). Rethinking phylogenetic comparative methods. *Systematic Biology*, 67(6), 1091–1109. <https://doi.org/10.1093/sysbio/syy031>
- Vizcaíno, S. F., & Loughry, W. (2008). *The biology of the Xenarthra*. University Press of Florida.
- Voje, K. L., Hansen, T. F., Egset, C. K., Bolstad, G. H., & Pélabon, C. (2014). Allometric constraints and the evolution of allometry. *Evolution*, 68(3), 866–885. <https://doi.org/10.1111/evo.12312>
- Wagner, G. P. (1996). Homologues, natural kinds and the evolution of modularity. *American Zoologist*, 36(1), 36–43. <https://doi.org/10.1093/icb/36.1.36>
- Weaver, T. D., Roseman, C. C., & Stringer, C. B. (2007). Were Neanderthal and modern human cranial differences produced by natural selection or genetic drift? *Journal of Human Evolution*, 53(2), 135–145. <https://doi.org/10.1016/j.jhevol.2007.03.001>
- Weidenreich, F. (1941). The brain and its role in the phylogenetic transformation of the human skull. *Transactions of the American Philosophical Society*, 31(5), 320–442. <https://doi.org/10.2307/1005610>
- Weston, E. M. (2003). Evolution of ontogeny in the hippopotamus skull: Using allometry to dissect developmental change. *Biological Journal of the Linnean Society*, 80(4), 625–638. <https://doi.org/10.1111/j.1095-8312.2003.00263.x>

- Wetzel, R. M. (1980). Revision of the naked-tailed armadillos genus *Cabassous* McMurtrie. *Annals of the Carnegie Museum*, 49, 323–357. <https://doi.org/10.5962/p.330852>
- Wetzel, R. M. (1985). Taxonomy and distribution of armadillos, Dasypodidae. In G. G. Montgomery (Ed.), *The evolution and ecology of armadillos, sloths, and vermilinguas* (pp. 23–46). Smithsonian Institution Press.
- Wible, J. R., & Gaudin, T. J. (2004). On the cranial osteology of the yellow armadillo *Euphractus sexcinctus* (Dasypodidae, Xenarthra, Placentalia). *Annals of the Carnegie Museum*, 73(3), 117–196. <https://doi.org/10.5962/p.316081>
- Wilson, L. A. (2018). The evolution of ontogenetic allometric trajectories in mammalian domestication. *Evolution*, 72(4), 867–877. <https://doi.org/10.1111/evo.13464>
- Wilson, L. A., & Sánchez-Villagra, M. R. (2010). Diversity trends and their ontogenetic basis: An exploration of allometric disparity in rodents. *Proceedings of the Royal Society B: Biological Sciences*, 277(1685), 1227–1234. <https://doi.org/10.1098/rspb.2009.1958>
- Zachos, F.E. (2020). Mammalian phylogenetics: A short overview of recent advances. In K. Hackländer, & F. Zachos (Eds.), *Mammals of Europe—Past, present, and future. Handbook of the mammals of Europe* (pp. 31–48). Springer. https://doi.org/10.1007/978-3-030-00281-7_6
- Zelditch, M. L., & Goswami, A. (2021). What does modularity mean? *Evolution and Development*, 23(5), 377–403. <https://doi.org/10.1111/ede.12390>
- Zelditch, M. L., Sheets, H. D., & Fink, W. L. (2003). The ontogenetic dynamics of shape disparity. *Paleobiology*, 29(1), 139–156. [https://doi.org/10.1666/0094-8373\(2003\)029<0139:todosd>2.0.co;2](https://doi.org/10.1666/0094-8373(2003)029<0139:todosd>2.0.co;2)
- Zelditch, M. L., & Swiderski, D. L. (2022). The predictable complexity of evolutionary allometry. *Evolutionary Biology*, 50(1), 56–77. <https://doi.org/10.1007/s11692-022-09581-1>